The Thesis Committee for Hamdi Ahmed Alramadan
Certifies that this is the approved version of the following thesis:

Experimental Evaluation of Surface Treated Nanoparticles and their Effect on Wettability Alteration of Carbonate Surfaces and Oil-Brine Interfacial Tension

APPROVED BY
SUPERVISING COMMITTEE:

Supervisor:

David A. DiCarlo

Kishore K. Mohanty

Experimental Evaluation of Surface Treated Nanoparticles and their Effect on Wettability Alteration of Carbonate Surfaces and Oil-Brine Interfacial Tension

by

Hamdi Ahmed Alramadan, B.S.

Thesis

Presented to the Faculty of the Graduate School of

The University of Texas at Austin

in Partial Fulfillment

of the Requirements

for the Degree of

Master of Science in Engineering

The University of Texas at Austin

August 2016

Dedication

To my loving parents, my wife, my brothers, my sisters, and my friends that made my life easier in tackling this challenge.

Acknowledgements

This work accentuates the fabulous motivation and support received at the University of Texas at Austin during my graduate studies period. A sincere appreciation and gratitude is expressed to my research advisor Dr. David DiCarlo for his continuous support and guidance throughout my studies. It is a must for me to emphasize the great level of organization and the continuous weekly advising session he provided, which helped me tackle various challenges in my research. In a nutshell, being a part of his team was of an utmost honor to me.

A great thankfulness is also forwarded to Dr. Kishore Mohanty for his valuable input and feedback in my research and for providing me the full privilege to use some of the necessary equipment that supported my studies. A special thank goes to Dr. Ijung Kim for his helpful guidance during my experimental work. An extended appreciation is directed to Dr. Mohammad Lotfollahi and my colleague Siddharth Senthilnathan for their useful comments and support. Another special thank goes to my fellow graduate student Shehab Alzobaidi from the Chemical Engineering department for his support in providing useful comments and experimental materials.

My deepest appreciation goes to my loving wife and family for their continuous support that allowed me to thrive in this interesting journey. A great appreciation and gratitude is expressed to my more than a cousin Yahya Alramadan and his wife for their support in various personal aspects. Finally, an extended thankfulness is expressed to Saudi Aramco management for the provided opportunity to pursue my advanced degree.

Abstract

Experimental Evaluation of Surface Treated Nanoparticles and their Effect on Wettability Alteration of Carbonate Surfaces and Oil-Brine Interfacial Tension

Hamdi Ahmed Alramadan, M.S.E.

The University of Texas at Austin, 2016

Supervisor: David A. DiCarlo

The alteration of rock surface wettability and the reduction of oil/brine interfacial tension enhances oil recovery from the reservoir. Most of the carbonate rock reservoirs around the world are oil-wet and changing their wettability may enhance oil recovery. Moreover, nanoparticles have presented a promising potential in enhanced oil recovery applications. An experimental study of contact angle changes upon exposure to nanoparticles on carbonate surfaces that are dispersed in brine solution has been conducted using various nanoparticle solutions, some of which were in-house synthesized. Also, interfacial tension measurements and calculations were implemented using the pendant drop method to study the effect of the invading nanoparticles solution. Nanoparticle concentrations were varied and progress was monitored with time. Effects of nanoparticle size, grafting coverage and mixed chemicals as well as observations are discussed. Two hypotheses were proposed for the wettability alteration mechanisms.

Table of Contents

List of Tables

List of Figures

Chapter 1: Introduction

This chapter presents the goal of this research and provides an outline for the remainder of the thesis document.

1.1 Goal of the Study

Based on the research done in the past, altering wettability toward water wetness tends to increase the overall oil recovery. As a great majority of the oil reservoirs around the world are carbonates that are mostly oil-wet, it is motivating to find efficient and economical means to change the rock surface wettability from oil-wet to water-wet in order to achieve higher oil recoveries. Moreover, reducing oil/brine interfacial tension has also proven to be effective in mobilizing oil which will potentially increase oil recovery. The significance of wettability and IFT alteration in enhancing oil recovery is discussed in depth in the chapter 2.

Various methods have been proposed to reduce interfacial tension and to change wettability such as the use of surfactants (Standnes and Austad, 2000; Rosen et al., 2005). Moreover, hydrophilic silica nanoparticle solutions are actively studied nowadays due to their promising potential that might provide a breakthrough in enhanced oil recovery and CO_2 sequestration applications (Roustaei et al., 2012; Aroonsri et al., 2013). No research was done to study the effects of various nanoparticle solutions on the carbonate surface wettability and the oil/brine interfacial tension. However, most of the nanoparticles research was done on sandstone surfaces and cores (Ju and Fan, 2009).

In this study, various nanoparticle solutions from commercial producers and synthesized in-house were experimented on to assess the efficiency of nanoparticle solutions in altering the carbonate surface wettability or the oil/brine interfacial tension which will ultimately enhance oil recovery. An understanding on the wettability and IFT

alteration mechanisms by nanoparticles should be gained at the end of the study. Also, an insight of the main affecting factors to be focused on whilst designing a specific nanoparticles solution would be gained such as the nanoparticles size, nanoparticles grafting components, and the chemicals in the carrying solution.

1.2 THESIS OUTLINE

This thesis contains five chapters in which background knowledge of the study aspects and experimental results of wettability and interfacial tension are covered. The second chapter presents a literature review regarding the fundamentals of wettability and interfacial tension along with some alteration techniques. It also discusses the latest research in which hydrophilic silica nanoparticles are of importance to the oil industry. The third chapter discusses the materials and methods of the experimental work done in this study. The fourth chapter provides the results of the wettability and interfacial tension experiments as well as a discussion section that analyzes the findings and observations and draws a conclusion of the possibility to perform any alteration using nanoparticles. Finally, the fifth chapter discusses the study results and provides recommendations for future work that will enhance the knowledge about nanoparticles potential and bring them closer to being applied successfully in the field.

Chapter 2: Literature Review

This chapter provides a brief background on the fundamentals of wettability and interfacial tension (IFT). All enhanced oil recovery affected parameters are covered as well as the developed means to alter both properties. Also, a review of nanoparticles and their potential effect on wettability and IFT are covered at the end of this chapter.

2.1 Enhanced Oil Recovery

Production from a reservoir can be categorized into three different phases depending on the stage of life and production requirements. These phases are called primary, secondary, and tertiary. The primary recovery phase is when the reservoir produces itself naturally using energy sources from within such as rock and fluid expansion, solution gas, water influx, gas cap, and gravity drainage. Moreover, the depletion of these energy sources presents the need to move to the secondary recovery phase which is achieved by the injection of external fluids for the purpose of maintaining reservoir pressure and enhancing volumetric sweep efficiency. External fluids may be water, gas or both.

During the secondary recovery phase, certain areas in the reservoir may be bypassed due to variations of permeability. Moreover, fingering due to variable fluid viscosities, channeling through natural or induced fractures, and/or coning of the injected fluid may leave significant amounts of oil behind. In addition, surface and interfacial forces contribute to trapping oil in reservoir pores in which it cannot be displaced by the injected fluid (Sheng, 2010). The abovementioned events necessitate the transition to the tertiary recovery phase to allow for higher oil recovery.

Tertiary recovery includes all enhanced recovery methods from injecting special fluids such as chemicals to injecting miscible gases or thermal energy into the reservoir.

Enhanced oil recovery is not restricted to the tertiary recovery phase as it can be implemented anytime during the life of the reservoir. Wettability alteration in carbonate rocks and the reduction of interfacial tension between oil and the displacing fluid will be the focus of study in this research.

2.2 ROCK WETTABILITY

Wettability is the fluid's tendency "to spread or adhere to a solid surface in the presence of other immiscible fluids". In reservoirs, rock surfaces may be covered with oil or water films depending on the wettability status and strength. Moreover, wettability is considered an essential factor affecting various parameters that are directly related to oil recovery. Fluids distribution and flow behavior in a reservoir can be controlled by the wettability condition. Moreover, wettability affects capillary pressures, relative permeability, electrical properties, and waterflood behavior (Anderson, 1986).

2.2.1 Reservoir Wettability Types

A reservoir can be water-wet, oil-wet, neutrally-wet, or a mix of all these three conditions. In a water-wet reservoir, the water tends to occupy smaller pores and contact the majority of rock surface. On the other hand, in an oil-wet reservoir, the oil tends to occupy smaller pores and contact the majority of rock surface.

If the rock surface would preferentially contact water as much as it would contact oil, the system is considered neutrally-wet. Moreover, the term fractional wettability is introduced for reservoirs where parts are strongly oil-wet due the adsorption of crude oil components while the remaining parts are strongly water-wet (Anderson, 1986).

It is worth mentioning that the reservoir rock wettability is not evaluated by the fluid currently in contact. However, it is evaluated by the rock surface preference to a certain fluid. For example, if a rock is fully saturated by oil, it is not necessarily true that

the rock is oil-wet as the rock surface is exposed to oil but it is still in preference to water. So, the wettability ambiguity should be better evaluated during the presence of both fluids (Anderson, 1986). Figure 2-1 illustrates the various wettability condition in the pore scale.

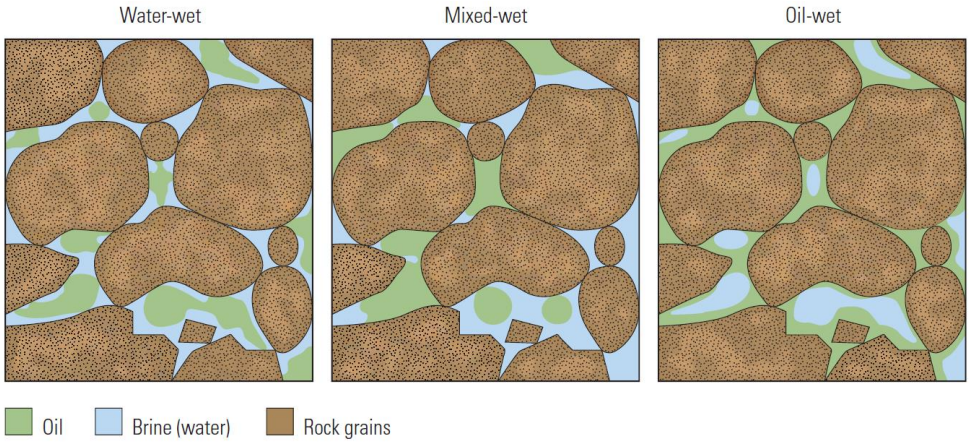

Figure 2-1: Wettability conditions illustration in the pore space (Schlumberger, 2007)

2.2.2 Original Reservoir Wettability

Throughout the history, it was believed that all petroleum reservoirs are water-wet as all clean sedimentary rocks are strongly water-wet. Moreover, sandstone reservoirs were deposited in aqueous environments and oil migrated afterwards which led to believe that the water would not allow the oil to contact rock surfaces. However, in 1937, some producing reservoirs were found to be strongly oil wet (Anderson, 1986). In fact, a study on 55 oil reservoirs showed that 67% of all reservoirs are oil-wet and 84% of the carbonate reservoirs are oil-wet, which indicate that a significant number of reservoirs are not water-wet (Treiber, 1972).

Reservoir original wetness alteration is attributed to several factors such as the adsorption of polar compounds or the deposition of organic matter from the crude oil. Polar compounds contain both a polar and a hydrocarbon end in which the polar end adsorbs on

the rock surface leaving the hydrocarbon end on the opposite side which will make the surface oil-wet. Experiments have shown that these compounds are sufficiently soluble in water allowing them to penetrate the original water film and render the surface oil-wet (Anderson, 1986). In addition, the degree to which wettability is altered is determined by pressure, temperature, mineral surface and brine chemistry.

Mineral surfaces are important in determining wettability. For example, carbonate reservoirs found to be more oil-wet than sandstone reservoirs due to the fact that the silica in sandstones have negatively charged weakly acidic surface while carbonates have positively charged weakly basic surface. The surface will adsorb compounds of opposite polarity by acid/base reaction (Anderson, 1986).

2.2.3 Wettability Affected Parameters

Understanding the wettability of a reservoir and performing analysis on cores with matching wettability is essential as wettability condition affects capillary pressure, relative permeability, dispersion, and electrical properties.

2.2.3.1 Effects on Electrical Properties of Porous Media

The Archie saturation exponent (n) seems to be affected by the wettability of the reservoir, especially, at lower brine saturations. In the case of a uniformly water-wet system, the saturation exponent would have a value of around 2 even at residual water saturations as the uniformity of water wetness allows for continuous electrical conduction through the thin water film. On the other hand, oil-wet formations would result in high exponent values up to 10 or more due the trapped brine that cannot contribute to the electrical conductivity. Failure to evaluate the formation at the appropriate wettability condition would severely affect the saturation calculations (Anderson, 1986).

2.2.3.2 Effects on Capillary Pressure

The capillary pressure and saturation relationship is dependent on the wettability interaction, pore structure, and saturation history. Whenever there is a curvature at the fluids' interface, the pressure will abruptly increase to balance the interfacial tension forces as given by Laplace's equation:

$$P_c = p_o - p_w = \sigma\left(\frac{1}{r_1} + \frac{1}{r_2}\right)$$

Generally, modeling a porous medium as a set of capillary tubes is not possible and an apparent contact angle is calculated from the displacement capillary pressure or the complete capillary pressure curve. Moreover, wettability and capillary pressure cannot be related by a simple expression to evaluate the capillary pressure at two different wettability conditions. However, capillary pressure data may be evaluated to realize the effect of wettability. Figure 2-2 shows capillary pressure curves for intermediate and strong water-wet scenarios.

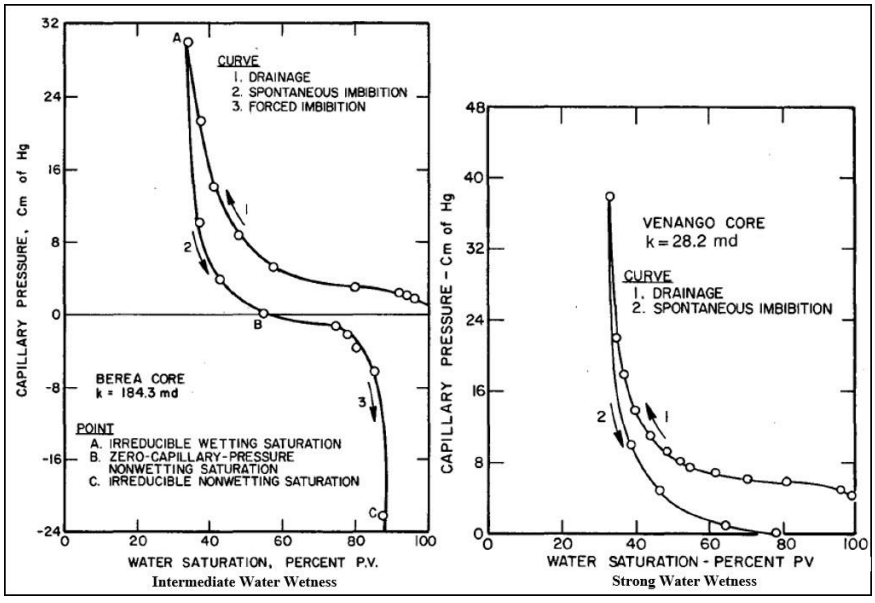

Figure 2-2: Capillary pressure curves for intermediate and strong water-wet scenarios (Anderson, 1987)

For each of the curves in Figure 2-2, the area under the curve is related to the work required for one fluid to displace the other fluid. By looking closely at the drainage curves for both scenarios, it is obvious that the area under the strong water-wet curve is greater than the area under the intermediate water-wet curve. This indicates that more work is required to displace water from the strong water-wet core. The opposite behavior is observed for the oil-wet case. The observed capillary pressure change with wettability urges us to analyze cores having wettability conditions similar to the native-state to ensure acceptable oil recovery estimations (Anderson, 1987).

2.2.3.3 Effects on Relative Permeability

Wettability affects relative permeability by controlling the flow and spatial distribution of fluids in a porous medium. The effective oil permeability seems to decrease at a given water saturation when the wettability is altered into being more oil-wet. On the other hand, the water relative permeability will increase with the wettability changing to an oil-wet condition (Anderson, 1987). Figure 2-3 illustrates the change in relative permeability with the wettability variation. The relative permeability curves in Figure 2-3 demonstrate that when a core is cleaned and its wettability is changed into a more water-wet condition, the water relative permeability decreases and oil relative permeability increases. This is an indication that serious relative permeability errors will occur if the core's wettability is not restored to the native-state prior to measurements.

2.2.3.4 Effects on Waterflooding

As wettability affects various essential parameters, waterflood and oil recovery estimations is greatly affected by the wettability condition. During a waterflood of a strong water-wet system, a significant percentage of the oil in place is recovered prior to breakthrough and the water cut increases rapidly afterwards and the residual oil saturation

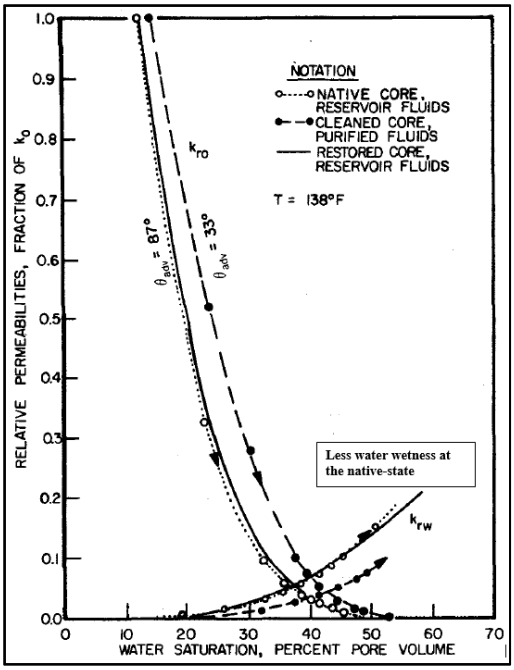

Figure 2-3: Illustrating change of relative permeability with wettability variation (Anderson, 1987)

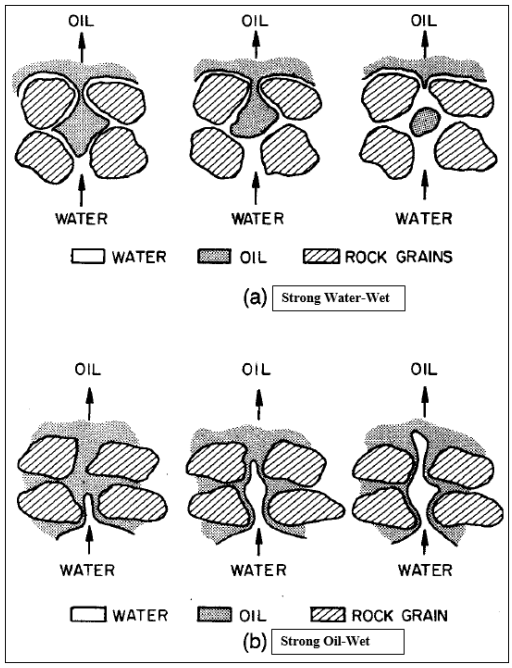

Figure 2-4: Pore Scale waterflood illustration for strong oil- and water-wet scenarios (Raza, 1968)

is low. Conversely, in a strong oil-wet system, the water will breakthrough earlier and most of the oil is recovered afterwards making the waterflood less efficient in this case as more water must be injected to recover the same amount of oil. Figure 2-4 illustrates the waterflood process for water- and oil-wet systems at the pore scale level. Figure 2-5 shows the oil recovery percentages along with the changes of wettability. It is obvious in the figure that the stronger the water-wetness, the higher the recovery is supposed to be (Anderson, 1987).

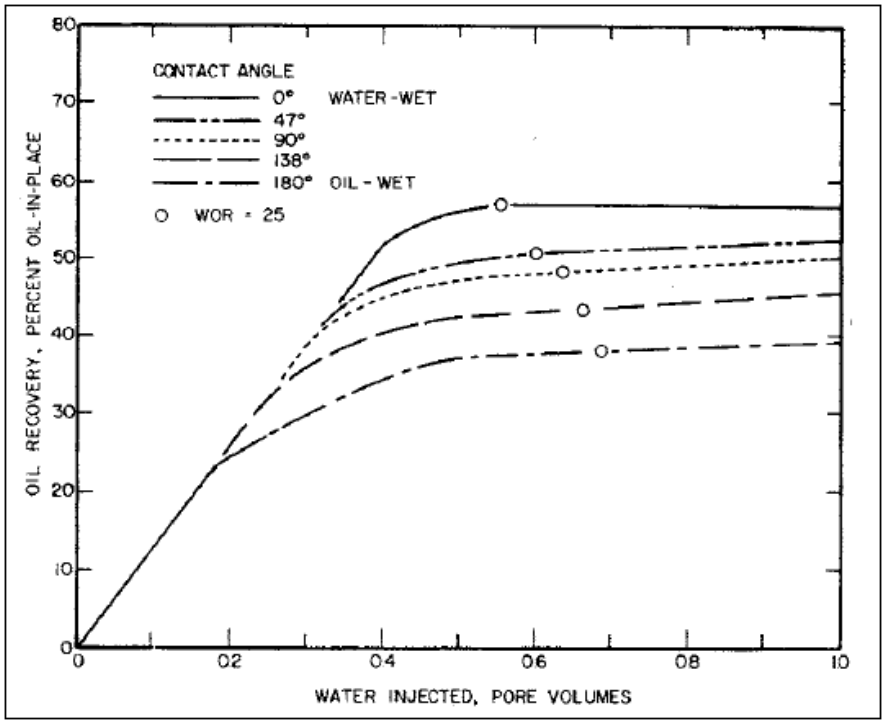

Figure 2-5: Oil recovery changes with wettability variations (Owens and Archer, 1971)

2.2.4 Wettability Alteration in Carbonates

Various approaches and techniques are used to alter wettability in carbonates. One approach is through changing the brine ionic composition. Active ions such as Ca^{2+}, Mg^{2+}, and SO_4^{2-} have been concluded to act as wettability modifiers in carbonates. At high

temperatures, the adsorption of Ca^{2+} onto the carbonate surface was noticed to increase along with the increase in adsorption of SO_4^{2-} which acts as a catalyst in the wettability alteration process. Both Ca^{2+} and Mg^{2+} adsorb on the surface during the process, however, Mg^{2+} shows higher adsorption at the higher end of temperatures. Figure 2-6 illustrates how these ions act to alter wettability on the carbonate surface (Austad, 2008).

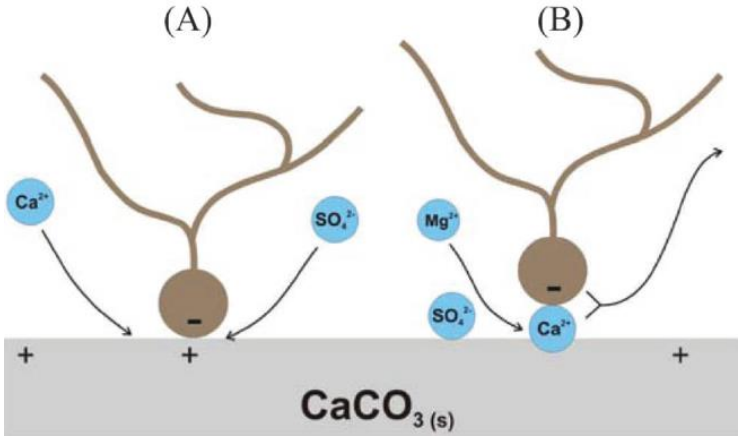

Figure 2-6: Wettability alteration by Calcium, Magnesium and Sulfate ions (Austad, 2008)

As illustrated in Figure 2-6, the adsorption of the sulfate ions decreases the positive charge of the surface which causes an excess of Ca^{2+} to be close to the surface. The Ca^{2+} reacts with the carboxylic groups present in the crude oil. At high temperatures, Mg^{2+} becomes active and it can displace the calcium-carbonate complexes from the surface (Austad, 2008). Moreover, high calcium/sulfate ratios are more effective in the wettability alteration in carbonates at high temperatures but within the solubility limit of $CaSO_4$ as it might precipitate and affect oil recovery severely. The precipitation of $CaSO_4$ is controlled by the presence of magnesium (Tweheyo, 2006).

Another approach into altering wettability in carbonates is by using low salinity brine for injection in high temperature and high salinity reservoirs. The contact angle measurements when introducing low salinity brines confirms the ability to change the wettability towards the water-wet state. Moreover, nuclear magnetic resonance (NMR) results indicated that the injection of different salinity slugs of brine in carbonates alters surface charges, which leads to more interactions with water molecules (Yousef, 2010).

One of the most proven and popular approaches to alter wettability of carbonates from oil-wet to water-wet is through the use of surfactants. Furthermore, various surfactant types are being used to alter wettability and improve spontaneous imbibition in carbonates such as cationic and anionic surfactants. One study showed that cationic surfactants seem to more effective in chalk reservoirs as they tend alter wettability in an irreversible way by desorbing organic carboxylates present in crude oil (Standnes, 2000).

Another study concluded that both anionic and cationic surfactants can help imbibing water into initially oil-wet capillaries but the anionic surfactant solutions were faster. Moreover, force adhesion analysis in the same study and contact angle measurements proved greater wettability alteration possibility with using anionic surfactants (Kumar, 2008).

In the later study, silicon and mica were used as substrates for the experiments while chalk was the rock used for the first study, which enlightens us to consider the circumstances. Surfactant properties that must be considered during the surfactant formulation design include critical micelle concentration value (CMC), hydrophobic property, interfacial tension value, and steric effects close to the N-atom. In addition, adsorption issues are usually encountered while using surfactants that can make them unattractive to some companies; however, the addition of some agents, such as sodium

carbonate alkaline in anionic surfactants, can significantly reduce surfactants adsorption on the carbonate rock surface (Zhang, 2006).

2.2.5 Wettability Measurement Techniques

Various methods can be used to evaluate wettability in quantitative or qualitative means. Quantitative methods include the direct measure of contact angles, imbibition and forced displacement test (Amott), and the USBM wettability method (Anderson, 1986). On the other hand, qualitative methods include imbibition rates, microscopic examination, flotation, glass slide method, relative permeability curves, permeability/saturation relationships, capillary pressure curves, capillarimetric method, displacement capillary pressure, reservoir logs, nuclear magnetic resonance, and dye adsorption. In this study, the focus is on contact angle measurements.

2.2.5.1 Contact Angle

One of the best techniques to evaluate wettability directly is through measuring contact angles of fluids on flat solid surfaces, especially when pure fluids and artificial cores are used to stronger control over the compounds that might alter wettability. Figure 2-7 shows a typical oil/water/solid system where the surface energies are related by Young's equation as follows:

$$\sigma_{ow} \cos \theta_w = \sigma_{os} - \sigma_{ws}$$

By convention, the contact angle is measured through the water but it can be measured through the oil as it is measured in this thesis. The sigma symbols represents the interfacial tension between each of the phases. Contact angles below 90° degrees indicate water wetness and angles higher than 90° indicate oil wetness. In addition, wettability becomes preferentially stronger when the contact angle is far away from 90°. In practice,

a system is considered neutrally or intermediately wet at angles ranging from 75° to 105°. Moreover, a water-wet system will have angles ranging from 0° to 75° and an oil-wet system will have angles ranging from 105° to 180°.

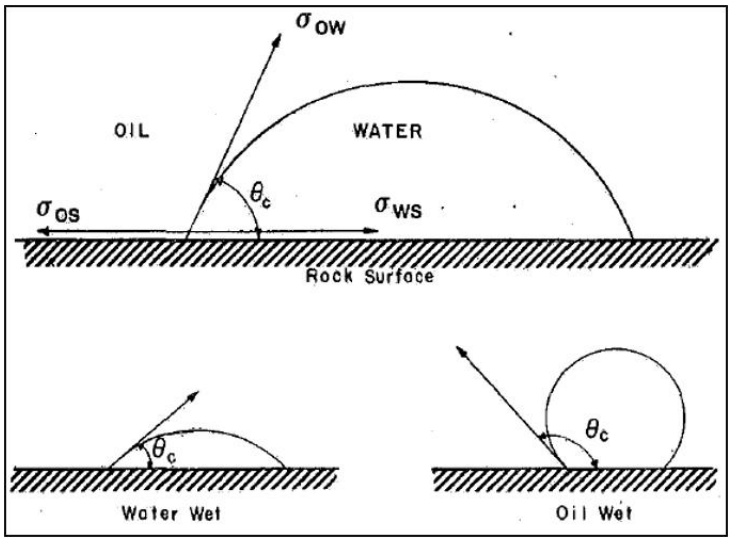

Figure 2-7: Contact angle and surface energies diagram (Raza, 1968)

Contact angle hysteresis might be faced during measurements due surface roughness, surface heterogeneity, and surface immobility on a macromolecular scale. As illustrated in Figure 2-8, the surface contact line will be affected on rough surfaces and false contact angles might be interpreted, so, smooth surfaces are always suggested to measure wettability. Furthermore, reservoir rock surface is heterogeneous which might affect contact angle measurements, which suggests the use of single mineral crystals instead. Also, the permanently present or absent organic coating on the reservoir rock might affect the proposed wettability condition. Considering these factors will help ascertain the representability of the measurements to the actual condition (Anderson, 1986).

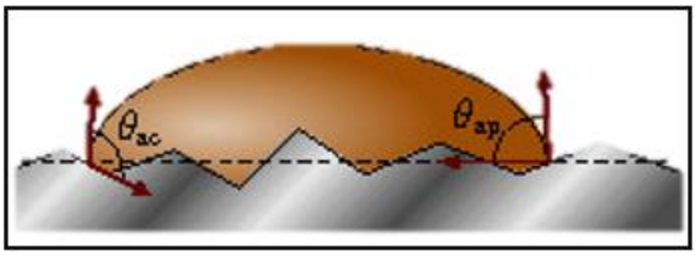

Figure 2-8: Actual and apparent contact angle on a rough surface. (Research Gate, 2007)

2.2.5.2 Other Wettability Measurements Techniques

Amott and USBM are the other two quantitative methods to measure wettability (Anderson, 1986). Both methods provide average wettability measurements of cores and each has its own pros and cons. The calculated wettability indices using both methods is related the spontaneous or forced drainage and imbibition of fluids into and out of the core.

Qualitative wettability measurement methods provide quick and rough idea about the wettability of the analyzed system without the need for the additional complication. On the contrary, there is a tendency that these methods might lead to false wettability judgments. For example, flotation methods simply require water, oil and sand to be placed in a glass bottle then shaken to observe the settling sand grains. If the system is water-wet, clean sand grains will be observed, and vice versa. However, this technique would only work in strong wettability cases as there are no means to evaluate intermediate wettability cases.

For the cases of fractional wettability when the system has portions with strong oil-wet surface while the rest is strongly water-wet, NMR and dye adsorption methods have been developed. The NMR method uses nuclear magnetic thermal relaxation time for water protons (hydrogen) in porous media and a relationship has been observed between wettability and the relaxation time. On the other hand, the dye adsorption method is based on the observation that a rock surface covered with water will adsorb large amounts of

methylene blue, whereas oil covered surface will not (Anderson, 1986). These methods remain qualitative and are controlled by various limitations.

2.3 INTERFACIAL TENSION

Interfacial or surface tension (IFT) is the force that holds the surface of a certain fluid together when another fluid exists. In oilfield, interfacial tension is usually reported in dynes/cm or mN/m and it is a function of pressure, temperature, and the composition of each fluid. Crude Oil-Brine interfacial tension values have been reported to be in the range of 25 to 35 mN/m (Firoozabadi, 1988).

Various experiments have been done on reservoir rock in order to determine the conditions required to remove residual oil, usually after a waterflood. In most of the cases, the oil removed seemed to be a function of the ratio $\Delta P/L\sigma$, where ΔP is the pressure drop across the distance L and σ is the interfacial tension between oil and water. No residual oil has been able to be displaced before exceeding a critical value of this ratio which appeared to be a fundamental rock property. Moreover, this ratio can be increased by applying more pressure or by lowering interfacial tension which can be achieved by using surface active agents (Taber, 1969).

In laboratory experiments on short cores, achieving high values of this critical displacement ratio was manageable by altering either of both variables and excellent recoveries of up 100% were accomplished. However, when scaling these results to ensure applicability in the field, pressure drop has to be increased so high above the formation fracture limit, which leaves no choice but to have an ultralow interfacial tension (Taber, 1969).

The idea of the capillary number was developed afterwards which correlated the critical displacement ratio with the sample permeability ($k_w\Delta P/L\sigma$). It was found that

residual oil recovery may be achieved if viscous forces acting on that oil exceed the capillary retaining forces ($\nu\mu/\sigma$) (Chatzis and Morrow, 1984). Both expressions contain interfacial tension.

The latest development of this ratio incorporated the capillary number and the bond number which takes into account the buoyancy forces on the fluid. A new number is defined as the trapping number (N_T) that has been shown to correlate very well with residual saturations of nonwetting, wetting and intermediate wetting phases in a wide variety of rock types (Pope, 2000). Figure 2-9 shows the results of decreasing wetting phase saturations with increasing trapping number values. In all of the abovementioned developments, reduction of IFT will increase the ratio.

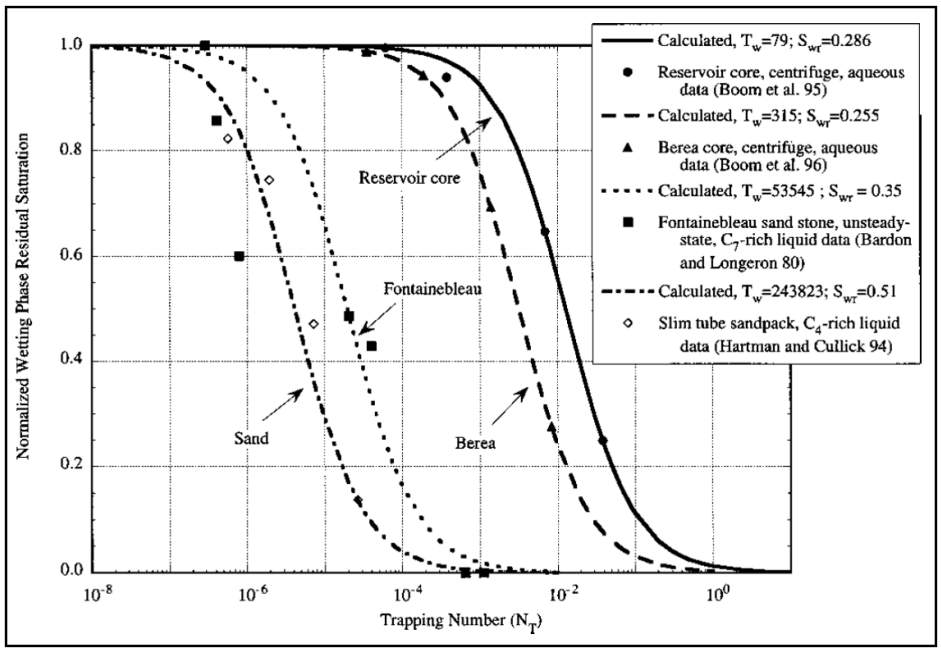

Figure 2-9: Trapping number desaturation curves of various rock samples (Pope, 2000)

2.3.1 Measuring IFT Using Pendent Drop Method

A needle is used to suspend a drop of a certain fluid in a bulk liquid or gaseous phase. Interfacial tension and gravity determine the shape of the drop. Moreover, pressure inside the drop phase increases as the interfacial tension between the outer and inner phase increase. In addition, the drop is deformed under the effect of gravity as the produced hydrostatic pressure due to the weight will control the drop main radii of curvature (KRUSS, 2016).

With the known densities of the drop and ambient fluids, the interfacial tension can be calculated using the following expression:

$$\sigma = \frac{g d_e^2 (\rho_d - \rho_a)}{H}$$

where d_e is the maximum diameter of the drop as shown in Figure 2-10, ρ_d is the density of the drop phase, ρ_a is the ambient fluid phase, H is a constant that is a function of $\frac{d_e}{d_s}$, and g is the gravitational acceleration. This method can be used for high pressures and temperatures (Peters, 2012).

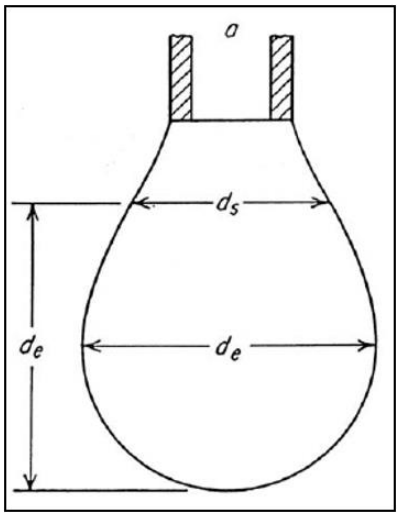

Figure 2-10: Pendant drop method schematic

2.4 SILICA NANOPARTICLES IN THE OIL INDUSTRY

Nanotechnology is the study of manipulating matter at the atomic and molecular scale. Moreover, a nanoparticle is the most fundamental component in the fabrication of a nanostructure with a diameter ranging from 1 to 100 nm (Horikoshi, 2013). Nanotechnology has attracted various researchers and companies in the oil industry due the substantial capabilities, especially in enhanced oil recovery applications. The promising capability of nanoparticles to modify magnetic, optical, and electrical properties makes them an interesting target to be field tested for EOR in the near future. Nanoparticles have this applicability to these various fields due to the fact that they can be tailored to any specific purpose by grafting different chemicals on the particles surface as well as using different particle sizes.

2.4.1 Effects of Nanoparticles on Wettability and Interfacial Tension

Various studies have shown promising results that nanoparticles can actually alter the rock wettability (Roustaei, 2012; Skauge, 2010; Ogolo, 2012; Roustaei, 2013; Ju, 2006, 2009). A study on polysilicon nanoparticles concluded that these particles have the potential for increasing pore scale displacement through the reduction of interfacial tension and wettability alteration. Moreover, wettability of sandstone has been noticed to be altered from water-wet to neutral-wet with only one measurement reported. Also, a reduction of water-oil IFT was observed to be from 26.3 mN/m to 2.55 to 1.75 mN/m when exposed to nanoparticles (Roustaei, 2012).

On another study comparing silica particles, polymer solutions, and colloidal dispersion gels (CDG), it was not affirmative that silica nanoparticles will alter the wettability; however, it was concluded that the adsorption of nanoparticles on solid surfaces may change the wettability into being more water-wet (Skauge, 2010). Moreover,

the addition of ethanol to silicon oxide nanoparticles has been observed to alter wettability and reduce interfacial tension as well as improve oil recovery, but the degree of alteration was not clearly specified (Ogolo, 2012).

An investigation of silica nanoparticles in carbonates that focused on finding the optimum nanoparticles' concentration concluded that the wettability of the rock is effectively changed to strongly water-wet condition due to the fast adsorption of nanoparticles on the surface. In contrary, the interfacial tension seemed to increase 26.5 mN/m to 38.4 mN/m (Roustaei, 2013). A similar conclusion was reached in a study of the mechanism of EOR using silica nanoparticles that the adsorption of nanoparticles may lead to wettability change (Ju, 2006). Additionally, a polished slice of sandstone was immersed in a silica nanoparticles solution then an infused water drop was observed to change into a more water-wet condition as the contact angle started reducing (Ju, 2009).

In an attempt to alter the rock wettability from strongly water-wet to intermediate-wet, polysilicon nanoparticles in ethanol was reported to alter wettability to the targeted condition. In addition, the oil-water IFT has been reduced using the same particles (Onyekonwu, 2010). Finally, a study on microfluidic structures that mimic pore-throat geometries concluded that the nanoparticles' effect is very similar to that of surfactants as they reduce the trapped oil size mainly by reducing IFT (Xu, 2015).

2.4.2 Nanoparticles Adsorption

Nanoparticles are two to three orders of magnitude smaller than typical pore throats which lead to and easy penetration trough the reservoir; however, physiochemical attraction between nanoparticles and the rock surfaces may still result in significant adsorption. Moreover, pH and salinity are critical factors in determining the nanoparticles solution retention and stability. Results of 200 column-flood and core-flood experiments

revealed maximum adsorption concentrations spanning six orders of magnitude. In addition, both reversible and irreversible adsorption of nanoparticles may occur (Zhang, 2015). In cases of severe adsorption, field applications may be jeopardized which triggers the need of more predictive work of the nanoparticles behavior.

The primary purpose of the abovementioned studies was to analyze the feasibility of utilizing nanoparticle solutions in EOR applications by focusing on the results of the core floods. Wettability and IFT measurements were only supplemental with no detailed analysis. There is no general trend concluded to which direction are these nanoparticles affecting wettability and IFT. Also, none of the nanoparticle studies included wettability measurements on carbonate surfaces. This study will focus on the effects of various nanoparticle solutions on wettability and IFT at various concentrations which will help in detecting the factors and the physics involved. As a result, the newly designed nanoparticle solutions will help altering wettability and interfacial tension to our favor.

Chapter 3: Materials and Methods

This chapter explains all experimental procedures and lists all materials used in this research. The main purpose of this study is to observe and analyze oil droplets contact angle changes on carbonate minerals in the presence of nanoparticles. Also, the effect of nanoparticles on interfacial tension is studied.

3.1 MATERIALS

3.1.1 Synthesized Brine

Synthesized API brine and sodium chloride (NaCl) brines were used in the experiments. The API brine was prepared using 8% NaCl and 2% calcium chloride by weight. The NaCl brine was prepared using 8% NaCl by weight. Deionized water was used to prepare the brine solutions. After encountering some nanoparticles stability problems with the API brine, the NaCl brine was used for the remainder of the experiments.

3.1.2 Model Oil

To ensure control and repeatability over all experiments, a model oil was prepared using n-decane and 1.5% by weight of cyclohexanepentanoic acid from Sigma-Aldrich. The n-decane is transparent which lead us to use a small pinch of a nonpolar red dye powder called Oil Red O from Sigma-Aldrich to color the oil phase. The amount of the added dye is not specified and it is up to the experimenter's discretion and the desired darkness of the color. Once the oil is fully saturated with the dye, any added amount of the dye powder will precipitate in the bottom of the container. The coloring of the oil phase allowed us to clearly observe oil droplets on the carbonate surface.

3.1.3 Nanoparticle Solutions

14 different silica nanoparticle solutions were used in the experiments. Nanoparticles were suspended in variable solutions with partially known chemical components. Disclosure of full chemical recipes for the solutions and the nanoparticles coating was not available due to confidentiality measures taken by the producing companies. Samples were provided by Nissan Chemical, NYACOL, company X, and the Chemical Engineering Department at UT Austin. Table 3-1 lists all used nanoparticles with the respective particles size.

Nanoparticle Solution	**Particle Size (nm)**	**Stock Concentration (wt. %)**
Nissan V-1	5	20
Nissan V-2	5	20
Nissan V-3.2	5	20
Nissan V-2	12	20
Nissan V-2	25	20
Nissan V-1	80	20
Nissan V-2	80	20
Company X - 100	5	18.09
Company X - C	5	19.77
Company X - B	5	17.85
Company X - D	5	19.73
NYACOL DP 9711	46	30.5
NX6+PEG (6-9 EO)	5	13.27
NX6+GLYMO	5	8.5

Table 3-1: Silica nanoparticle solutions used in the experiments

3.1.4 Calcite Mineral

Calcite mineral plates ($CaCO_3$) from Ward's Science were used to represent carbonates rock surface in the experiments. These plates ranged in size from 1"x1" to 1"x2" and the surface of these plates was smooth with negligible roughness which required no polishing. Figure 3-1 shows a sample of the used calcite plates.

Figure 3-1: A sample of the used calcite plates (Ward's Science, 2016)

3.1.5 Cubic Quartz Cuvettes

Cubic glass cells that are chemically resistant with extremely low thermal expansion levels from Hellma-Analytics were used to contain the ambient solutions and the submerged calcite plates during the experiments. Teflon stands were fabricated in the Petroleum and Geosciences Department workshop to lift the calcite plates and allow for bottom drop analysis. Figure 3-2 shows schematics of the used cuvette and Teflon stands. It is necessary to note the capacity of the used cuvette as it is needed to avoid liquid overflow during the fluid addition. The cuvettes used in the experiments have a capacity of 88 ml.

Volume:	88000 µl
Outer Dimensions:	
Height:	52,5 mm
Width:	55 mm
Depth:	55 mm
Inner Dimensions:	
Height:	50 mm
Width:	50 mm
Depth:	50 mm

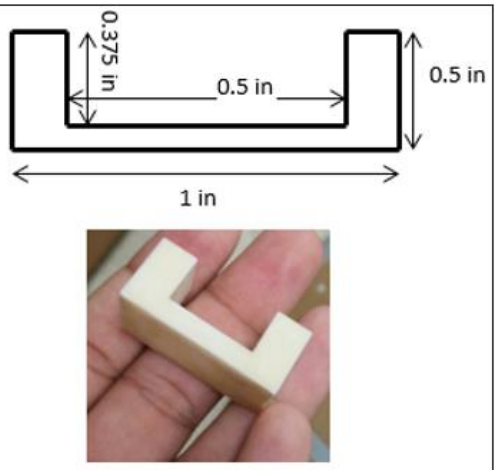

Quartz Cell | Teflon Stand

Figure 3-2: Schematics of the glass viewing cell (Hellma-Analytics) and the Teflon stand

3.1.6 pH Reduction Agent

Diluted hydrogen chloride (HCl) was used as a pH reducing agent for the cases were nanoparticles solution lose stability at high pH values when exposed to the various brines. A 1.21M HCl is used in the experiments which is diluted by a factor of 10 from a stock molarity of 12.1M. Small amounts of HCl were added when needed to avoid the alteration of the intended nanoparticles concentrations. The HCl is added after adding the nanoparticle solution to the cuvette in which the calcite plate is submerged.

Some nanoparticle solutions will increase the system's pH which will cause the particles to fall off solution and form a gel-like layer at the bottom of the cuvette. In some instances, only a foggy layer will appear at the bottom due to the low severity of nanoparticles aggregation but the solution will still be considered instable. That will affect the capability of the added nanoparticles to change the wettability or the interfacial tension. For nanoparticle solutions illustrating instability issues, reducing the pH value to lower than 6 seemed to have solved the problem. The added HCl amounts did not generally exceed 0.1 ml in the 88 ml cuvette when needed.

3.2 EQUIPMENT

The wettability and interfacial tension were measure using a Ramé-Hart goniometer/tensiometer as illustrated in Figure 3-3. It basically consists of a focus camera, an illumination source, and an adjustable middle base with a mounting arm. The instrument comes with an advanced software called DROPimage that calculates both contact angle and interfacial tension through the method of axisymmetric drop shape analysis. Moreover, ImageJ which is an open source image processing program was used to measure contact angles especially for the cases with lack of clear contrast around the drop perimeter.

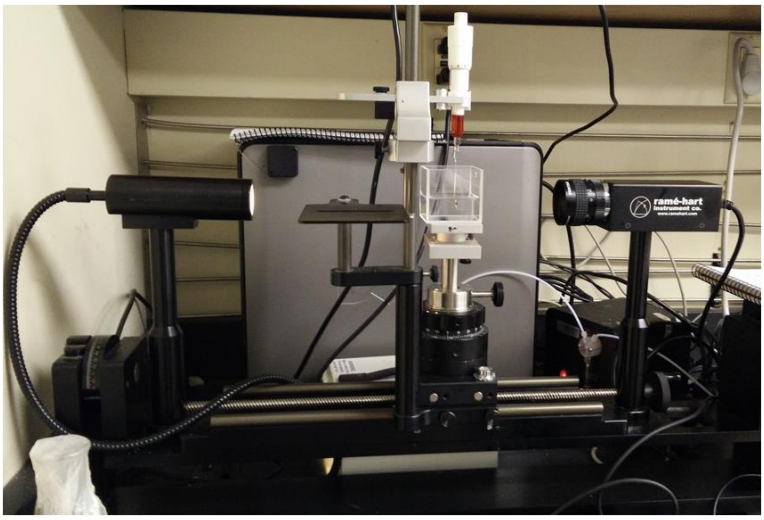

Figure 3-3: Ramé-Hart goniometer/tensiometer

For precise liquid volume additions and withdrawals, Eppendorf Research Plus pipettes with different volume limits were used to balance the desired solution concentrations. Also, a portable Oakton multipurpose meter was used for pH measurements. Figure 3-4 shows both of these two equipment.

Oakton pH meter	Eppendorf Research Plus pipettes

Figure 3-4: Volume transfer and pH measurement equipment (OAKTON and Eppendorf)

3.3 WETTABILITY EXPERIMENTAL PROCEDURE

For the purpose of the study as it is desired to analyze whether an oil-wet carbonate can be changed into a water-wet carbonate, the calcite plates' wettability was changed to oil-wet. The calcite plates were aged in brine then in the model oil for at least one day at room temperature. The added cyclohexanepentanoic acid in the model oil would adsorb on the positively charged mineral surface which will render the surface oil-wet (Gupta, 2008).

After aging the calcite plate in the model oil, the plate is transferred using a tweezer to a cuvette that is filled with known brine volume. The plate is submerged in the brine and is placed on a Teflon stand that is centered in the cuvette as shown in Figure 3-5. Oil drops should begin forming on the top and the bottom calcite surface from the attached oil layer due to the previous aging in oil. In case no oil droplets have formed on the calcite surface, an inverted needle can be used to place an oil drop at the bottom of the calcite surface. An equilibrium time is required to reach the final contact angle for the formed drop. It was

observed that one hour is more than sufficient to reach the final drop contact angle in which angle changes afterwards are not measurable.

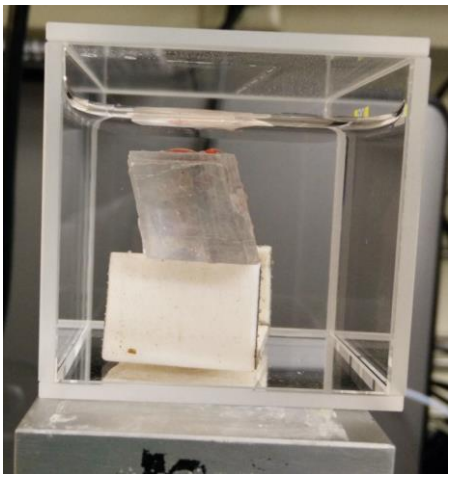

Figure 3-5: An aged calcite plate submerged in brine solution

Due the volume limitation of the used cuvette which has a volume of 88 ml, some of the brine in the cuvette might have to be withdrawn and replaced with the necessary amount of the stock nanoparticle solution in order to achieve. The calcite plate should remain submerged all the time during the experiment to avoid exposure to air which might affect the reached equilibrium contact angles. The following mass balance equation was used to calculate the required stock nanoparticles volume in order to achieve the desired final solution concentration:

$$V_1 \times C_1 + V_2 \times C_2 = V_3 \times C_3$$

where V_1 and C_1 are the initial brine volume and the nanoparticles concentration, respectively. The subscript "2" indicates the stock nanoparticles solution volume and concentration and the subscript "3" indicates the final solution volume and concentration.

Moreover, liquid withdrawal and injection was done slowly to avoid oil drops disturbance in order to clearly observe the effect of nanoparticles on wettability. In

addition, oil drops disturbance might occur by moving the cuvette on the goniometer base by hand; however, using the built in up-and-down and side-to-side handles helps to smoothly scan oil drops without significantly disturbing them. The top drop provides the water-advancing contact angle and the bottom drop provides the water-receding contact angle as the oil drop was placed afterwards and the oil is moving onto the mineral surface. The ambient solution should be clear and transparent and any sign of gelling or fogginess indicate the nanoparticles instability. Adding HCl to reduce the solution's pH after adding the nanoparticle solution was found to be helpful in sustaining the nanoparticles stability when needed. The experiments where nanoparticles instability was observed were repeated at lower pH conditions to observe changes in contact angles and rule out the solution instability factor.

For every experiment, a control set of oil drops were selected and captured after reaching equilibrium and before exposing them to nanoparticles. The contact angles calculated in experiments are the water phase contact angles which means that oil-wet conditions are determined when the contact angle is above 90°. The goniometer DROPimage software can measure the contact angle by defining the base and symmetry axes. In the cases of image contrast issues, the contact angle is measured manually using the ImageJ software. A total of 18 wettability experiments were performed of which different nanoparticles solution were used. The wettability change experiments included a combination of effects versus time and nanoparticles concentrations.

3.4 Interfacial Tension Experimental Procedure

The pendent drop method is used to calculate interfacial tension in all of the experiments in this study. The same cuvettes used in the wettability experiments were used here. The suspended drop was chosen to be an oil drop and the ambient fluid is the brine

or the nanoparticles solution. The oil phase is constant and the ambient phase is variable. Due to gravity effect and that oil is lighter in weight than water, the straight down needle is not appropriate for the pendent drop method. An inverted needle was connected to the drop dispenser as shown in Figure 3-6. The oil and brine densities must be accounted for in the DROPimage software to calculate accurate IFT values, see Table 3-2.

After suspending the upward drop, the needle tip horizontal axis and the symmetry vertical axis should be aligned prior to starting IFT measurements. The IFT was measured for 12 nanoparticles samples against time. Moreover, concentrations were varied for each sample to analyze the IFT alteration severity against nanoparticles concentration.

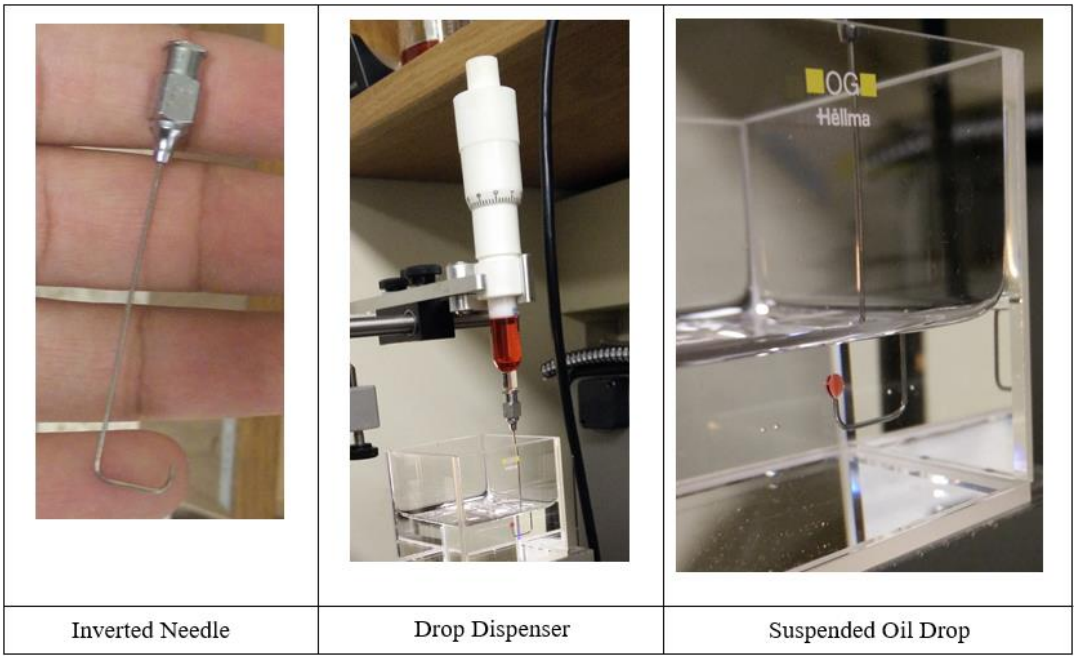

Inverted Needle	Drop Dispenser	Suspended Oil Drop

Figure 3-6: Inverted needle setup for the pendent drop method

Fluid	Density (g/ml)
Model Oil	0.73
8% NaCl Brine	1.06

Table 3-2: Model oil and brine properties

3.5 Oil Drop Behavior Experimental Procedure

The inverted needle used in the IFT experiments was used to infuse oil drops in a brine solution mixed with nanoparticles to observe the oil drops coalescence behavior. Only Nissan V-1 nanoparticles and the synthesized nanoparticles with polyethylene glycol were used in this experiment.

Chapter 4: Results and Discussion

This chapter includes the results of two sets of experiments. The first set involves 18 experiments of wettability alteration on carbonates using nanoparticles. The second set includes 12 oil/water interfacial tension reduction experiments using nanoparticles as well. The last section of the chapter discusses the overall results of the experiments.

4.1 Wettability Alteration Experiments

Suspended silica nanoparticle solutions were used in all wettability alteration experiments. The majority of the nanoparticles samples were provided by commercial producers. Two samples were synthesized by the chemical engineering department at the University of Texas at Austin.

4.1.1 Experiment 1: 1% Nissan 5 nm V-1

API brine was used in this experiment as the ambient medium. For the first experiment, the submerged calcite plate was left for 24 hours to monitor the contact angle changes in brine only in order to evaluate the equilibrium time. It was observed that after approximately 1 hour, no changes in the contact angle are occurring. Figure 4-1 illustrates the oil wet condition with the oil drop having a contact angle of 155.5° that did not change after 24 hours.

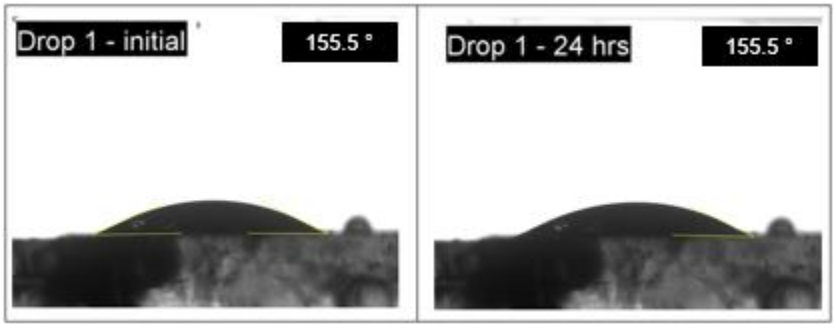

Figure 4-1: Oil drop in API brine after reaching equilibrium

Nissan 5 nm V-1 nanoparticles solution was used in this experiment. The concentration was adjusted to 1% while the calcite plate is submerged in the brine solution. As illustrated in Figure 4-2, there was no noticeable change in contact angle over the course of 24 hours. The contact angle was around 155.5° after the injection of the nanoparticles. The change was only 1.5° from the control case.

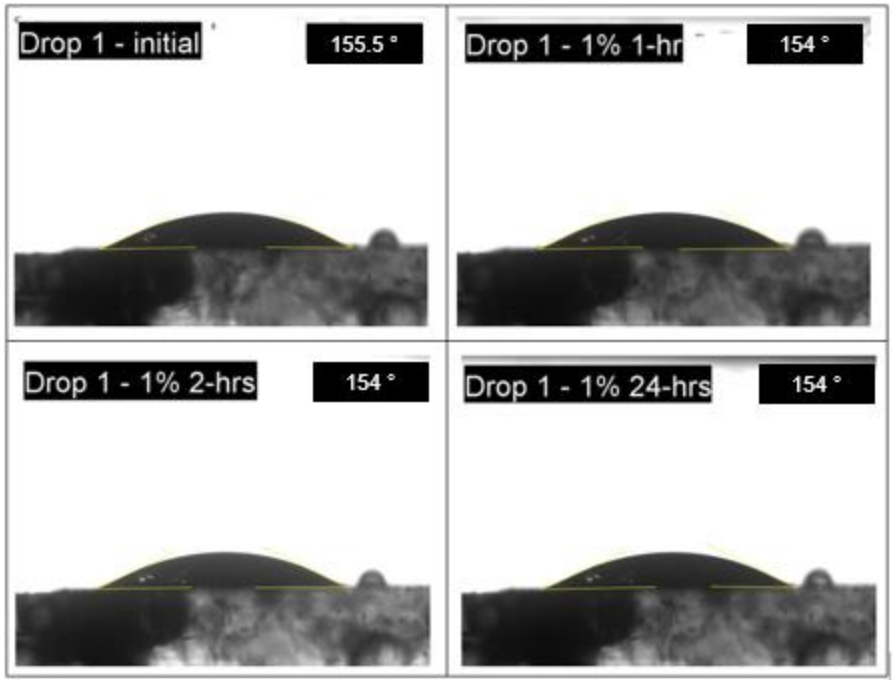

Figure 4-2: Contact angle changes with 1% Nissan 5 nm V-1 nanoparticles

The contact angle indifference is attributed to the nanoparticles solution instability issues at this experiment's conditions. The nanoparticles have fallen off solution after injecting them into the brine. Figure 4-3 shows progress pictures of the nanoparticles after injection. The solution was clear instantly after injecting the nanoparticles into the cuvette; however, the bottom of the cuvette started becoming cloudy within one hour of adding the

nanoparticles. After 24 hours, a thick gel-like layer have formed at the bottom where all nanoparticles have conglomerated.

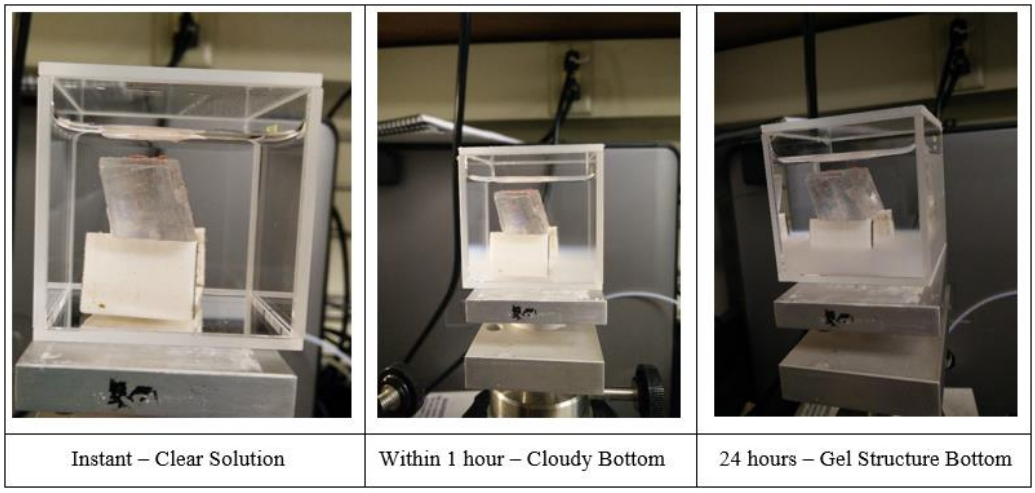

Figure 4-3: Nanoparticles falling off solution after injecting 1% Nissan 5 nm V-1

For the next experiments, it was decided to only use NaCl brine as the calcium in the API brine has been suspected to cause the instability issues.

4.1.2 Experiment 2: 1% Nissan 5 nm V-2

The aged calcite plate was submerged in 8% NaCl brine to eliminate the possibility of nanoparticles accumulation at the bottom and losing stability. After reaching equilibrium in the brine solution as shown in Figure 4-4, drop 1 formed an angle of 125.7° along with some areas on the side having flat oil films which indicate an oil-wet condition.

Within 1.5 hours of raising 1% concentration of the Nissan 5 nm V-2 nanoparticles, drop 1 contact angle reduced to 102.6° which sets this drop to be in the intermediate wettability condition. On the other hand, the flat thin oil films changed into multiple oil drops with contact angles ranging from 27.1° to 51.8° which indicates a strong water-wet condition. There was slight cloudiness at the bottom of the cuvette after injecting the

nanoparticles, see Figure 4-5. This cloudiness did not increase with time during the experiment.

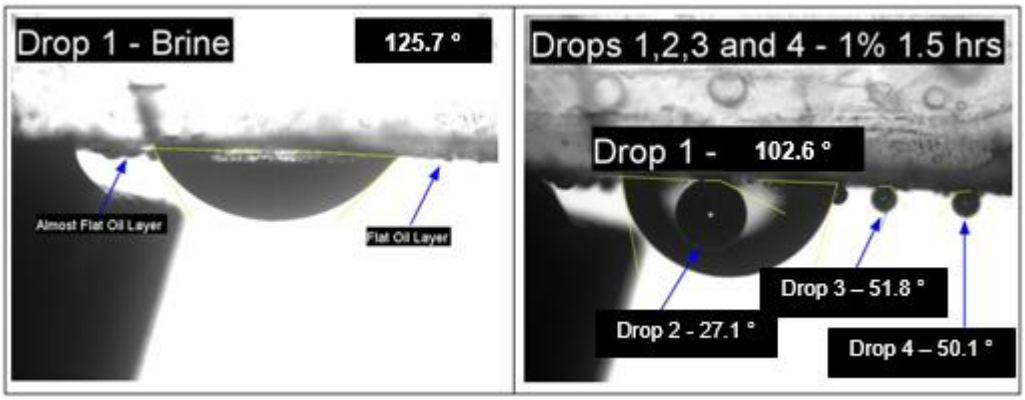

Figure 4-4: Contact angle changes with 1% Nissan 5 nm V-2 nanoparticles

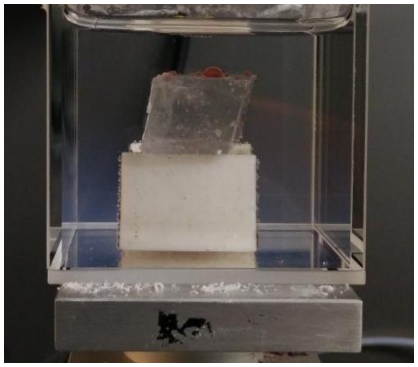

Figure 4-5: Slight cloudiness after injecting 1% Nissan 5 nm V-2 nanoparticles

4.1.3 Experiment 3: 1% Nissan 5 nm V-3.2

In this experiment, a drop at the bottom of the submerged calcite plate was placed using an inverted needle. Two drops were monitored for wettability changes after the injection of nanoparticles, drop 1 on the top and drop 2 on the bottom.

As shown in Figure 4-6, drop 1 have changed from oil-wet condition with a contact angle of 117.9° to an intermediate wet condition with a contact angle of 86.3°. Conversely,

drop 2 have an opposite behavior where the wettability have changed from being slightly water-wet after placing the oil drop to being slightly oil-wet after injecting the nanoparticles solution.

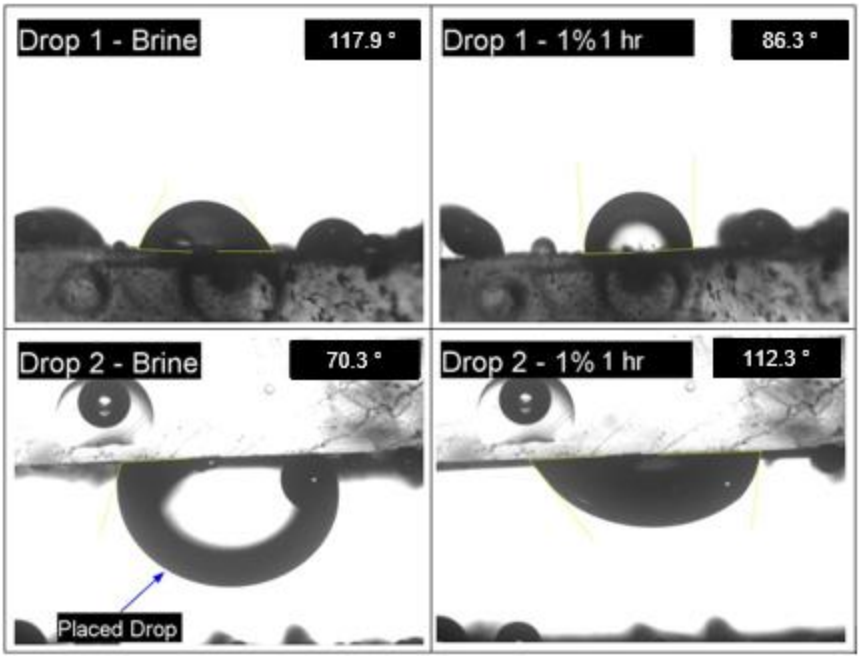

Figure 4-6: Contact angle changes with 1% Nissan 5 nm V-3.2 nanoparticles

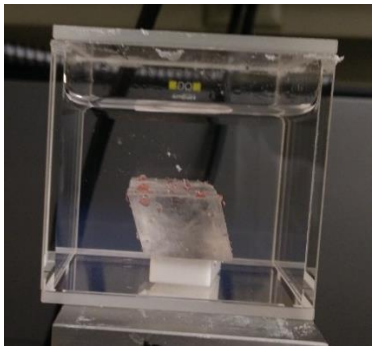

Figure 4-7: Slight cloudiness after injecting 1% Nissan 5 nm V-3.2 nanoparticles

A slight fogginess is appearing at the bottom of the cuvette as shown in Figure 4-7. The intensity of this foggy layer did not increase with time indicating that no further conglomeration of the nanoparticles might occur.

4.1.4 Experiment 4: 1% Nissan 12 nm V-2

The size of the nanoparticles used in this experiment is bigger than what was used in the first three experiment (12 nanometer particles vs. 5 nanometer particles); however, the chemical components in the solution and the particles coating is the same as the Nissan version 2 nanoparticles products. The formed oil drops showed an oil-wet condition after reaching equilibrium with contact angles ranging from 117.5° to 134.4°.

Wettability did not seem to be altered significantly after injecting 1% nanoparticle solution. Drops 1 and 2, shown in Figure 4-8, did not change into being water-wet. The contact angle changed minimally with a range from 3° to 8°. The oil drops have been monitored for more than two hours after injecting nanoparticles.

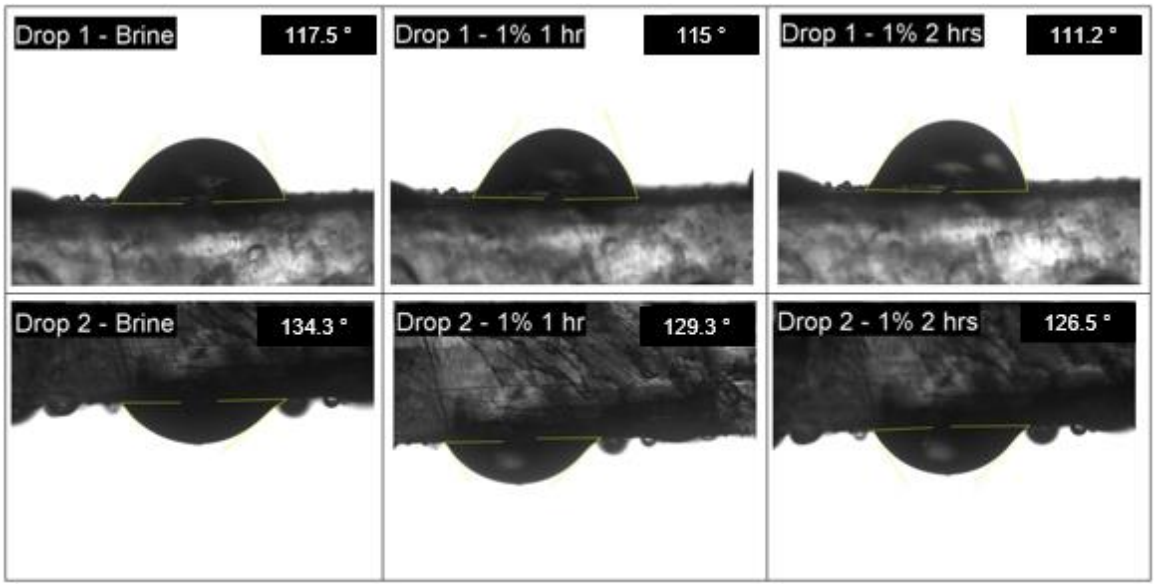

Figure 4-8: Contact angle changes with 1% Nissan 12 nm V-2 nanoparticles

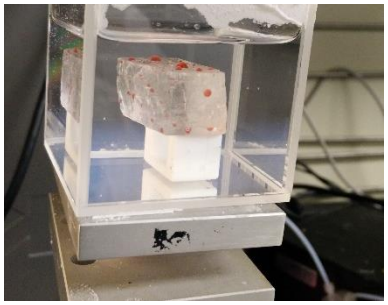

Figure 4-9: Slight cloudiness after injecting 1% Nissan 12 nm V-2 nanoparticles

As shown in Figure 4-9, slight cloudiness at the bottom of the cuvette indicates a small level of nanoparticles instability. The cloudiness intensity did not increase with time.

4.1.5 Experiment 5: 1% Nissan 25 nm V-2

The nanoparticles used in this experiment are 25 nanometer in diameter which is bigger than the nanoparticles used in experiment no. 4, but they have the same version 2 mixture from Nissan. After submerging the aged calcite plate and reaching equilibrium, the formed oil drops illustrated an oil-wet condition with angles ranging from 125° to 137.4°.

The wettability did not change significantly after adding 1% of the nanoparticles solution, see Figure 4-10. The oil drops were still showing an oil-wet condition after more than one hour of exposure to nanoparticles with angles at 112.1° and 120.8° for drops 1 and 2, respectively. Stronger cloudiness appeared at the bottom of the cuvette, which is attributed to the greater nanoparticles size as they tend to show less transparency due to the high number of light reflections between the particles, see Figure 4-11. This cloudy layer did not increase in intensity with time.

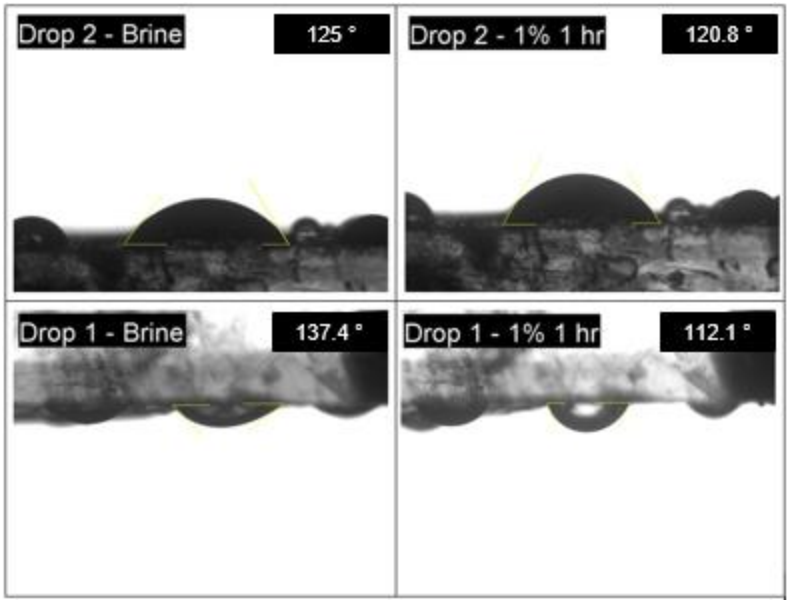

Figure 4-10: Contact angle changes with 1% Nissan 25 nm V-2 nanoparticles

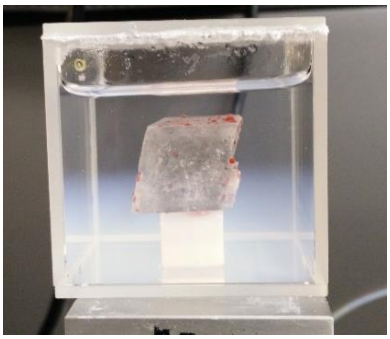

Figure 4-11: Cloudiness after injecting 1% Nissan 25 nm V-2 nanoparticles

4.1.6 Experiments 6 & 7: 1% Nissan 80 nm V-1 and V-2

Nanoparticles with diameters of 80 nanometer were used in experiments 6 and 7. The two experiments were combined in this section due to the fact that no wettability alteration observation were accomplished. The calcite plates were not visible after adding the nanoparticles as the solution was cloudy due to the big nanoparticles size. As shown in Figure 4-12, the stock nanoparticle solutions have a milky white color. Moreover, the 1% diluted nanoparticle solutions in the cuvette did not allow the submerged calcite plates to

be visible during the experiments. The big diameter of the particles causes so many light reflections that result in the solution's white color. The nanoparticles appeared to be stable in both experiments with minimal signs of aggregation.

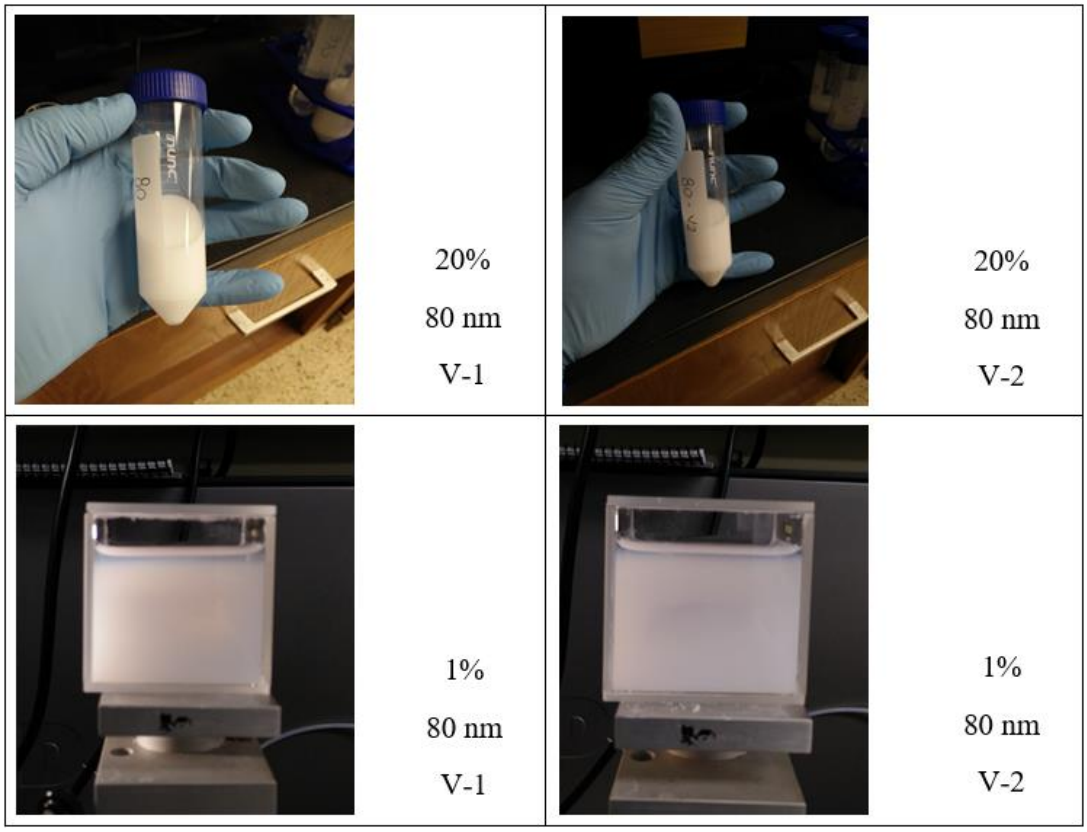

Figure 4-12: Stock and diluted 80 nm Nissan nanoparticles (V-1 and V-2)

The slight signs of nanoparticles aggregation encouraged to seek for a solution to the problem as ensuring full nanoparticles stability is key to successful fluid displacement. It was suggested that lowering the brine-nanoparticle solutions pH below 6 enhances the nanoparticles stability and ensures that all particles are suspended uniformly in the carrying fluid. Small amounts of HCl were used to lower pH in the following experiments.

4.1.7 Experiment 8: 1% Company X-100

Company X actual name will not be revealed due to an agreement between the company and the Petroleum and Geosystems department at the University of Texas at Austin. The nanoparticles in this sample have an average diameter of 5 nm. Two drops, drop 1 and drop 2, were monitored for wettability changes in this experiment. After reaching equilibrium state in the brine solution, drop 1 and drop 2 had contact angles of 110° and 72.5°, respectively as shown in Figures 4-13 and 4-14.

The pH of the solution after adding 1% of the nanoparticles was 9.5. Approximately, 1 ml of diluted HCl with 0.0121 M molarity was added to the system to lower its pH; however, the added 1 ml of the diluted acid did not seem to be effective in reducing its pH. The acid dilution by a factor of 1000 is the reason why the pH is not reduced with the added acid volume. Moreover, higher acid volumes will be required to achieve the desired pH; however, adding more acid will compromise the solution's salinity and nanoparticles concentration. The solution appeared to be clear with no signs of nanoparticles aggregation. As a result, it was decided to continue the experiment with no further pH adjustment and a higher molarity HCl (1.21 M) was used in the following experiments.

The added 1% nanoparticles have shown instant results on drop 1 and drop 2. Drop 1 has instantly snapped off as shown in Figure 4-13 and a thin oil film with a contact angle of 164.8° remained on the surface. Within 1 hour, this contact angle changed to 150°. Drop 2 was more in the intermediate wettability range and the contact with the added nanoparticles caused the drop to snap off instantly with no remaining oil on the calcite surface as shown in Figure 4-14.

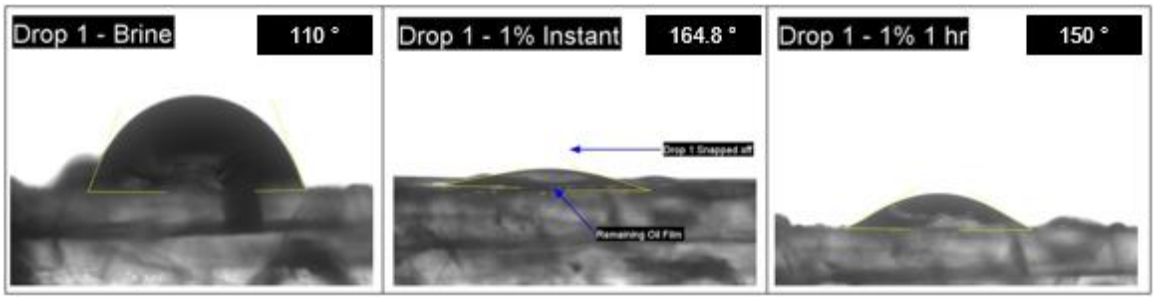

Figure 4-13: Contact angle changes with 1% Company X-100 (Drop 1)

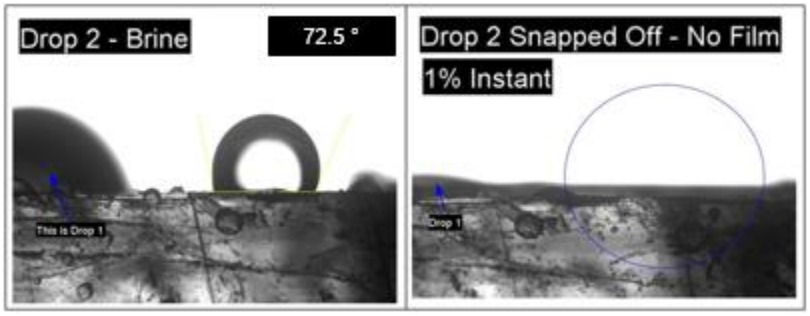

Figure 4-14: Contact angle changes with 1% Company X-100 (Drop 2)

4.1.8 Experiment 9: 1% Company X-C

Two drops were monitored after submerging the calcite plate and reaching equilibrium. Drop 1 had an equilibrium in-brine contact angle of 113.3° and drop 2 had a contact angle of 114.6°, which indicate an oil-wet condition of the calcite plate. After adding 1% of the Company X-C nanoparticles, the pH of the solution increased from 8.7 to 9.2 and then decreased to 2.52 after adding 0.5 ml of 1.21 M HCl. The added nanoparticles have an average diameter of 5 nm.

As shown in Figure 4-15, drop 1 snapped off instantly after adding the nanoparticles and the contact angle reduced to 75°. The contact angle reduced to 60.6° within 1 hour. Drop 2 contact angle reduced to 68° within 1 hour after adding the nanoparticles as well. The contact angles of both drops 1 and 2 after adding the nanoparticles solution indicate the change in wettability of the calcite plate surface to water-wet.

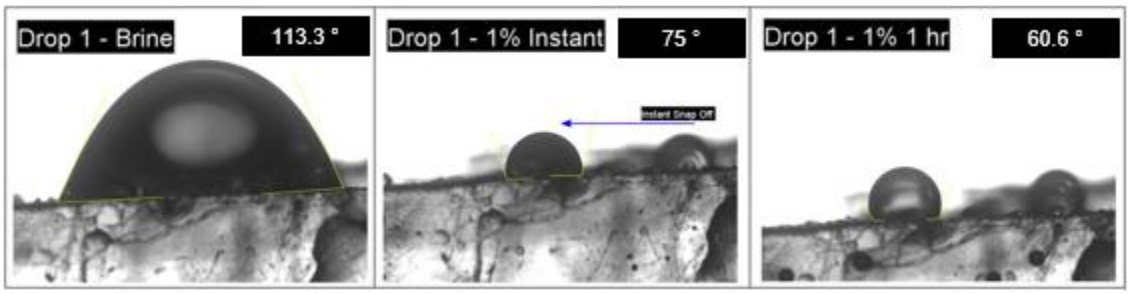

Figure 4-15: Contact angle changes with 1% Company X-C (Drop 1)

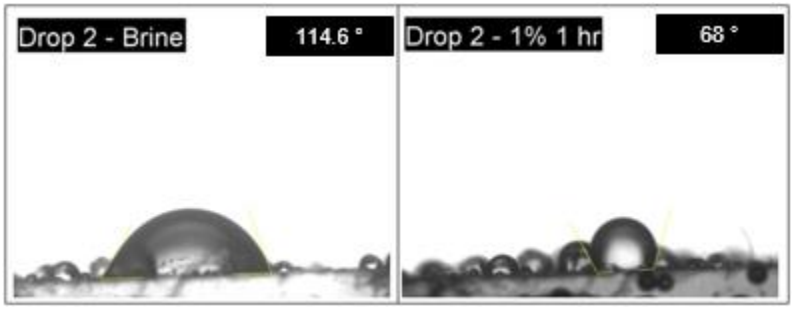

Figure 4-16: Contact angle changes with 1% Company X-C (Drop 2)

4.1.9 Experiment 10: 1% Company X-B

The nanoparticles in this sample have an average diameter of 5 nm. After submerging the calcite plate and reaching equilibrium, 1% of the Company X-B nanoparticles solution was added and the pH of the solution became 9.1. The solution became slightly cloudy after adding 0.2 ml of 1.21 M HCl, but this cloudiness faded away and the solution became clear after some gentle stirring and the pH became 7.5. Furthermore, another 0.2 ml of HCl was added to further reduce the pH. The pH of the solution reduced to 3.7; however, the whole solution became cloudy and the nanoparticles aggregated at the top of the calcite plate and the bottom of the cuvette with time as shown in Figure 4-17. Some drops were noticed to snap off after the addition of the nanoparticles

solution but no contact angles were measured due to the vision obstruction caused by the aggregated nanoparticles.

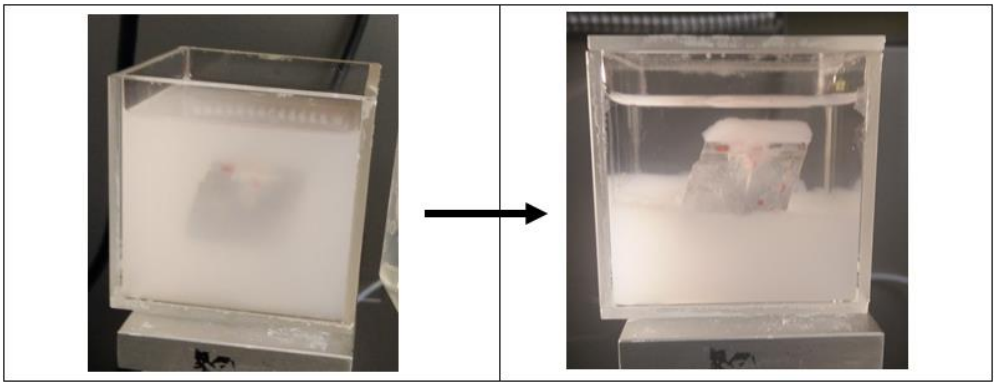

Figure 4-17: Company X-B nanoparticles aggregation after lowering pH

4.1.10 Experiment 11: 1% Company X-D

The reached equilibrium state in the brine solution resulted in contact angles higher than 90° for three oil drops that has been monitored throughout the experiment. The submerged calcite plate was confirmed to be in oil-wet condition. Moreover, the used nanoparticle solution in this experiment was from Company X-D with nanoparticles having an average diameter of 5 nm. As shown in Figure 4-18, the added 1% of the nanoparticles solution caused drop 1 to instantly snap off and a thin oil film remained on the calcite surface with a contact angle of 164.7° that did not significantly change over time.

Additionally, drop 2, shown in Figure 4-19, contact angle has changed instantly after adding the nanoparticles solution and within 1 hour, the contact angle decreased to 56°. Moreover, drop 2 snapped off the calcite surface within 4 hours of adding the nanoparticles solution, which indicate the wettability alteration to water-wet condition.

Also, drop 3 has snapped off instantly after adding the nanoparticles solution and the remaining oil formed a contact angle of 123° that reduced to 108° within the hour. The

contact angle has ultimately reduced to 62.5° within 4 hours of adding the nanoparticles. The contact angles changes for drops 2 and 3 indicate the wettability alteration from oil-wet to water-wet condition. The solution was very clear with no particles aggregation.

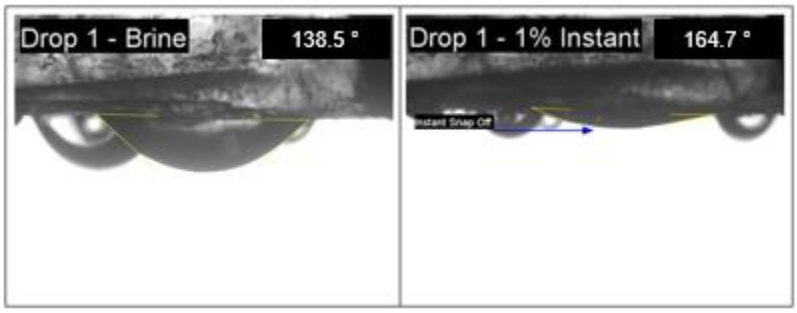

Figure 4-18: Contact angle changes with 1% Company X-D (Drop 1)

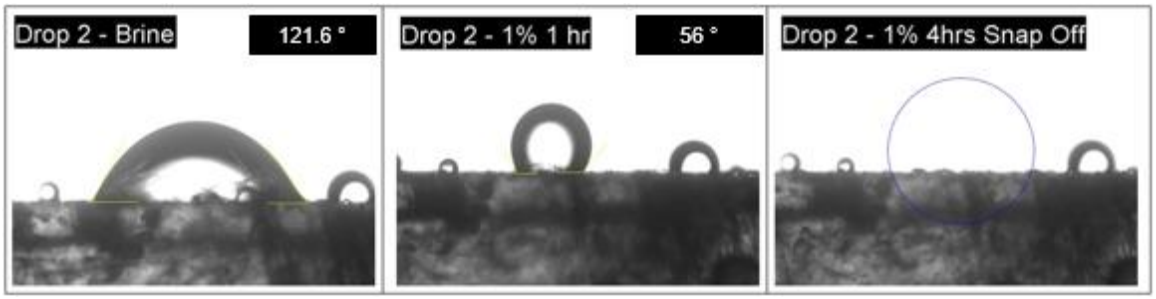

Figure 4-19: Contact angle changes with 1% Company X-D (Drop 2)

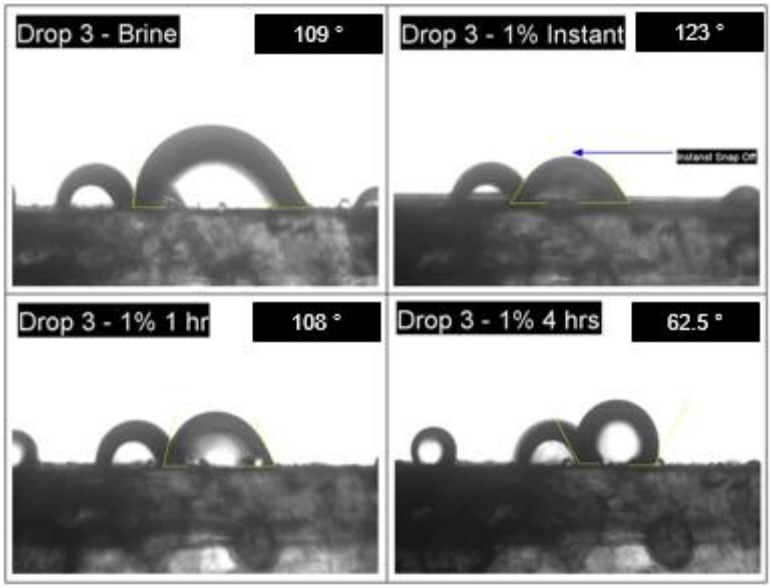

Figure 4-20: Contact angle changes with 1% Company X-D (Drop 3)

4.1.11 Experiment 12: 1% NYACOL DP 9711

The used nanoparticles in this NYACOL sample have an average diameter of 46 nm. After reaching equilibrium and confirming oil-wet state on the calcite plate, the added nanoparticles seemed to be slightly unstable at first as some cloudiness appeared in the cuvette. However, with some gentle stirring, the cloudiness cleared and the nanoparticles regained full stability. The nanoparticles sample was acidic and the addition of 1% of this sample caused the solution's pH to reduce to 4.75.

As shown in Figure 4-21 and Figure 4-22, the contact angle change was insignificant over time after adding the nanoparticles sample. Drop 1 contact angle has reduced by only 15° over a period of 4 hours. On the other hand, drop 2 contact angle has reduced by only 8° over a period of 4 hours. Since all contact angles were above 90° after adding the nanoparticles, the wettability remained unchanged in oil-wet condition.

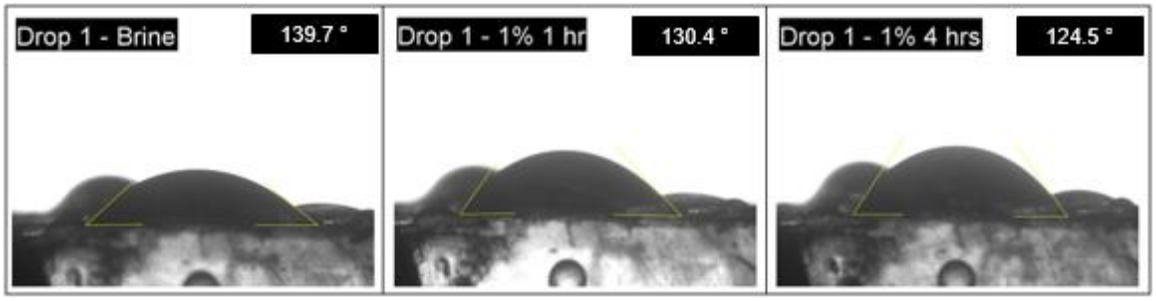

Figure 4-21: Contact angle changes with 1% NYACOL DP 9711 (Drop 1)

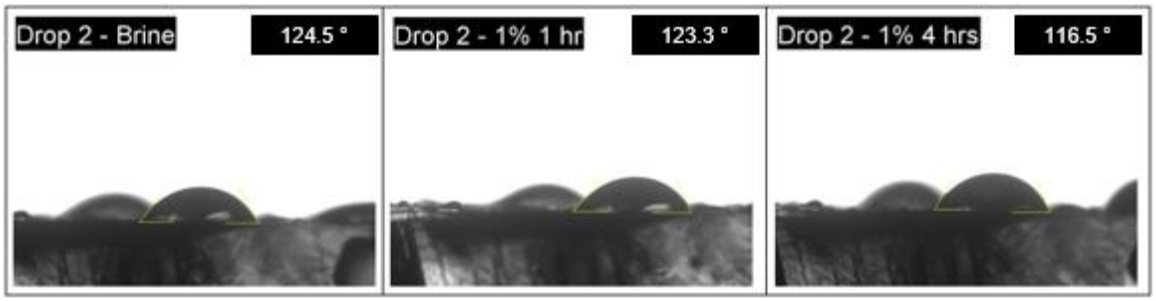

Figure 4-22: Contact angle changes with 1% NYACOL DP 9711 (Drop 2)

4.1.12 Experiment 13: 1%, 3% and 5% Nissan 5 nm V-1

Starting at this experiment, the wettability change observation was done using three different nanoparticles concentrations, 1%, 3%, and 5%. Two drops were monitored for contact angle changes in this experiment, see Figure 4-23 and Figure 4-24. Drop 1 contact angle has reduced from 141° to 99.6° after 1% of the Nissan V-1 nanoparticles. Furthermore, the contact angle reduced to 88.6° after increasing the nanoparticles concentration to 3%. With a concentration of 5%, drop 1 snapped of the calcite plate surface.

For drop 2, the contact angle changed to 86° and 80.8° with 1% and 3% concentrations, respectively. Drop 2 was snapped off with 5% nanoparticles concentration and the remaining oil film formed a small drop with a contact angle of 86°.The contact

angle change was higher between 3-5% than between 1-3% nanoparticles concentrations. The solution's pH was reduced to values below 6 by adding minimal amounts of 1.21 M HCl than don't exceed 0.1 ml at every nanoparticles concentration. The solution was stable.

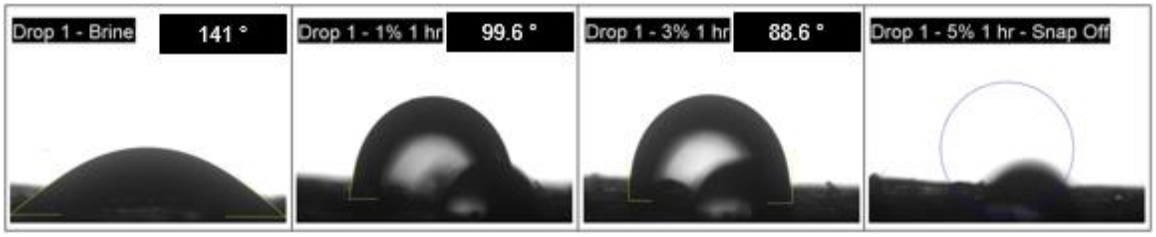

Figure 4-23: Contact angle changes with 1 to 5% Nissan 5 nm V-1 nanoparticles (Drop 1)

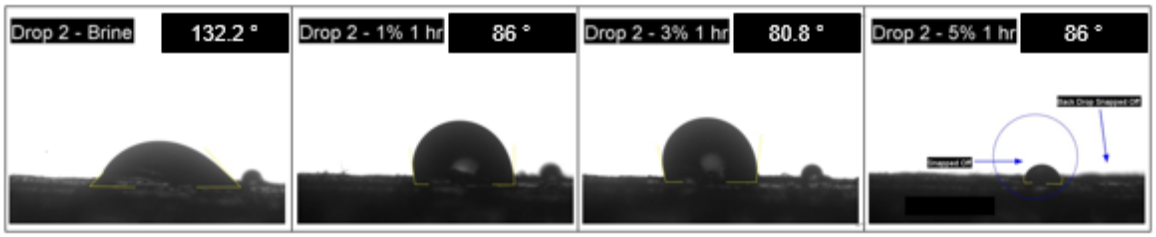

Figure 4-24: Contact angle changes with 1 to 5% Nissan 5 nm V-1 nanoparticles (Drop 2)

4.1.13 Experiment 14: 1%, 3% and 5% Nissan 5 nm V-2

Two formed drops were monitored for contact angle changes after reaching equilibrium in brine, see Figure 4-25 and Figure 4-26. After adding 1% of the Nissan V-2 nanoparticles, Drops 1 contact angle changed to 118.6°. Note that the sides of drop 1 were cut off and the drop size reduced. Increasing the nanoparticles concentration to 3% caused drop 1 contact angle to reduce to 67.4°. Moreover, drop 1 snapped off and the remaining oil film formed a drop with a contact angle of 131.4° after increasing the concentration to 5%.

On the other hand, drop 2 snapped off from the middle after adding 1% of the nanoparticles and the contact angle increased to 123°. In addition, increasing the nanoparticles concentration to 3% reduced the contact angle by only 8°; however, the drop snapped off the calcite plate with 5% nanoparticles concentration. The solution's pH was reduced to values below 6 by adding minimal amounts of 1.21 M HCl than don't exceed 0.1 ml at every nanoparticles concentration. The nanoparticles were stable in the solution.

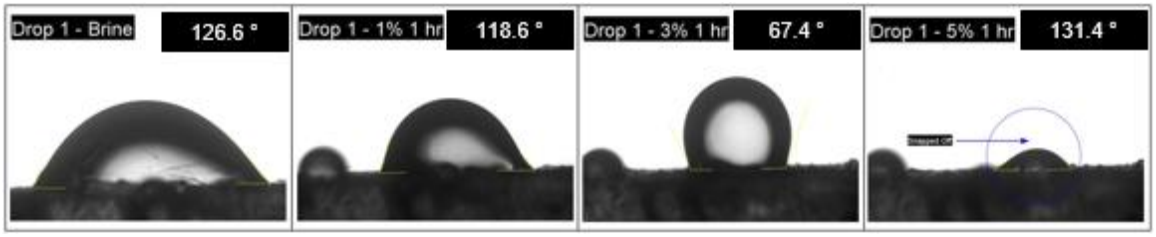

Figure 4-25: Contact angle changes with 1 to 5% Nissan 5 nm V-2 nanoparticles (Drop 1)

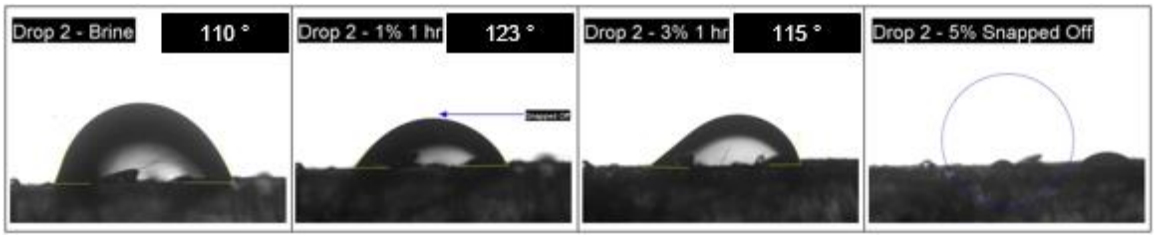

Figure 4-26: Contact angle changes with 1 to 5% Nissan 5 nm V-2 nanoparticles (Drop 2)

4.1.14 Experiment 15: 1%, 3% and 5% Nissan 5 nm V-3.2

Two drops were monitored in this experiment as well, see Figure 4-27 and Figure 4-28. The contact angle of drop 1 reduced to 76.8° after adding 1% Nissan V-3.2 nanoparticles. Furthermore, drop 1 snapped off the calcite plate surface after increasing the nanoparticles concentration to 3%. On the other hand, drop 2 kept snapping off and shrinking in size at every nanoparticles concentration increase. At the end, a small portion

of drop 2 remained and formed a contact angle of 154°. The solution's pH was reduced to values below 6 by adding minimal amounts of 1.21 M HCl than don't exceed 0.1 ml at every nanoparticles concentration. The nanoparticles were stable in the solution with no signs of aggregation.

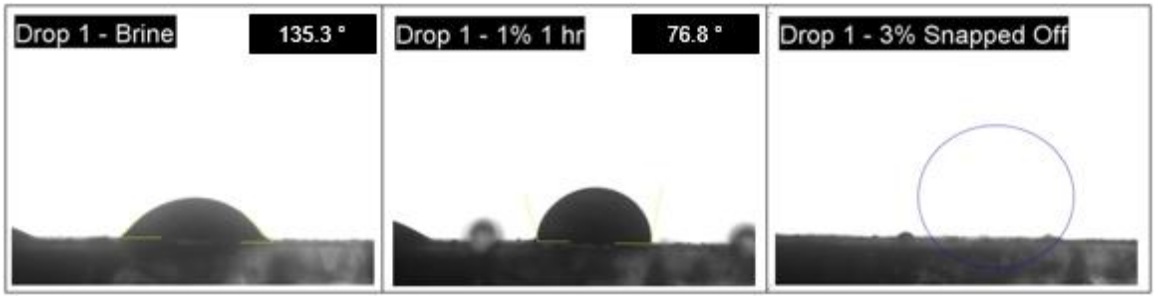

Figure 4-27: Contact angle changes with 1 to 3% Nissan V-3.2 nanoparticles (Drop 1)

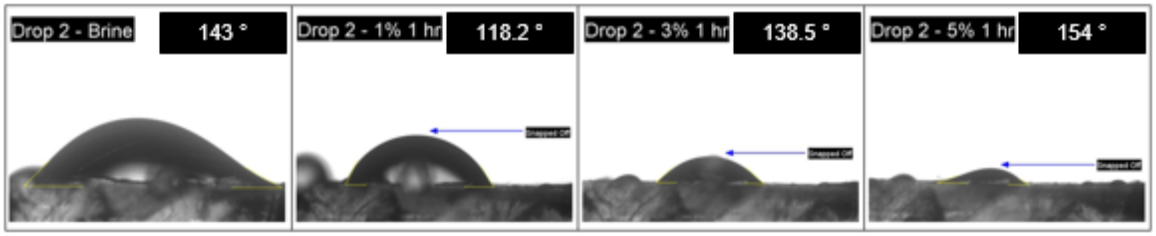

Figure 4-28: Contact angle changes with 1 to 5% Nissan V-3.2 nanoparticles (Drop 2)

4.1.15 Experiment 16: 1%, 3% and 5% Company X-D

Company X-D nanoparticles have an average diameter of 5 nm. The chosen two drops to be monitored reached contact angles of 135.6° and 137°, which indicate oil-wet condition. As shown in Figure 4-29 and Figure 4-30, the contact angles did not significantly decrease within 1 hour of adding 1% nanoparticles to the brine solution. Increasing the nanoparticles concentration to 3% caused both drops to snap off where drop 1 left a small trace and drop 2 snapped off the calcite plate surface completely. Moreover, raising the

concentration to 5% removed the remaining oil trace from drop 1 and snapped off the remaining oil drops on the back side of drop 2. Since the used sample here is from Company X, the pH reduction was unnecessary to ensure nanoparticles stability as observed in experiment 11.

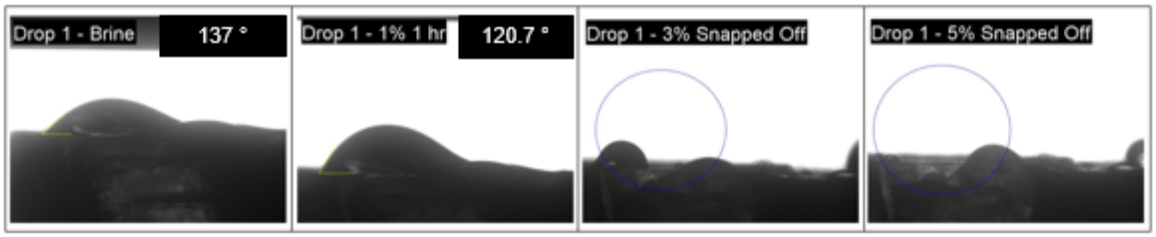

Figure 4-29: Contact angle changes with 1 to 5% Company X-D nanoparticles (Drop 1)

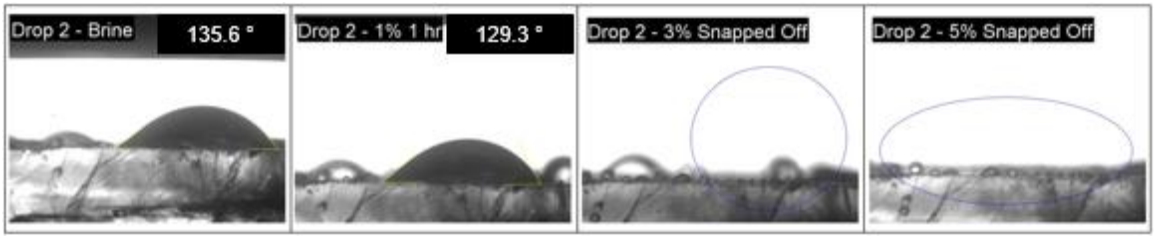

Figure 4-30: Contact angle changes with 1 to 5% Company X-D nanoparticles (Drop 2)

4.1.16 Experiment 17: 1% UT Synthesized NX6+PEG (6-9 EO)

To better understand the factors affecting wettability on the rock surface and due to the confidentiality measures taken by the commercial producers of nanoparticle solutions, it was decided to use some nanoparticle solutions that were synthesized at the University of Texas at Austin. The sample used in this experiment was prepared using NexSil 6 nm silica nanoparticles that were coated with polyethylene glycol that has a repeat unit of 6-9. The coating of the particles increases the diameter to around 18 nm. The brine solution

consisted of only 8% NaCl and the wettability change measurements were taken at room temperature as well.

The contact angle change was observed without reducing the solution's pH as the nanoparticles were stable and no signs of aggregation appeared. As shown in Figure 4-31, the addition of 1% of the nanoparticles solution snapped off the relatively big drop that was formed in the brine solution and approximately one third of that drop remained on the calcite surface with a contact angle of 148°. The contact angle kept reducing slowly until it stabilized at 97.3° within 3 hours of adding the nanoparticles. The measured contact angle indicates intermediate wetness condition.

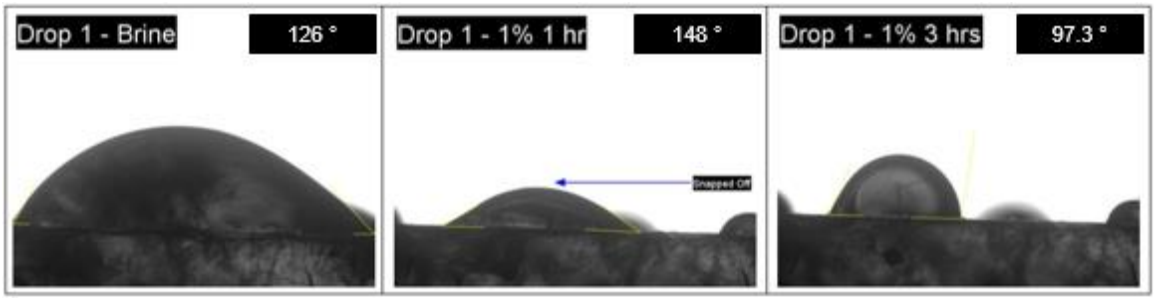

Figure 4-31: Contact angle changes with 1% UT Synthesized NX6+PEG nanoparticles

4.1.17 Experiment 18: 1% UT Synthesized NX6+GLYMO

The synthesized nanoparticles solution in this experiment was prepared using NexSil 6 nm silica nanoparticles that were coated with GLYMO. The coating of the particles increases the diameter to around 9 to 16 nm. Similar to experiment 17, the brine solution consisted of only 8% NaCl and the wettability change measurements were taken at room temperature.

Two drops were monitored in this experiment for contact angle changes. Drop 1 showed a strong oil-wet condition with a contact angle of 160° after equilibrium in the

brine solution. Raising the nanoparticles concentration to 1% around the submerged calcite plate did not seem to affect the contact angle of drop 1 over time. On the other hand, drop 2 did show some change in contact angle, but the change was insignificant as the contact angle changed by only 15° from 126.3° in the brine to 110.6° after adding the nanoparticles, see Figure 4-32. The pH of the solution was not reduced as the nanoparticles seemed to be stable and no signs of aggregation appeared.

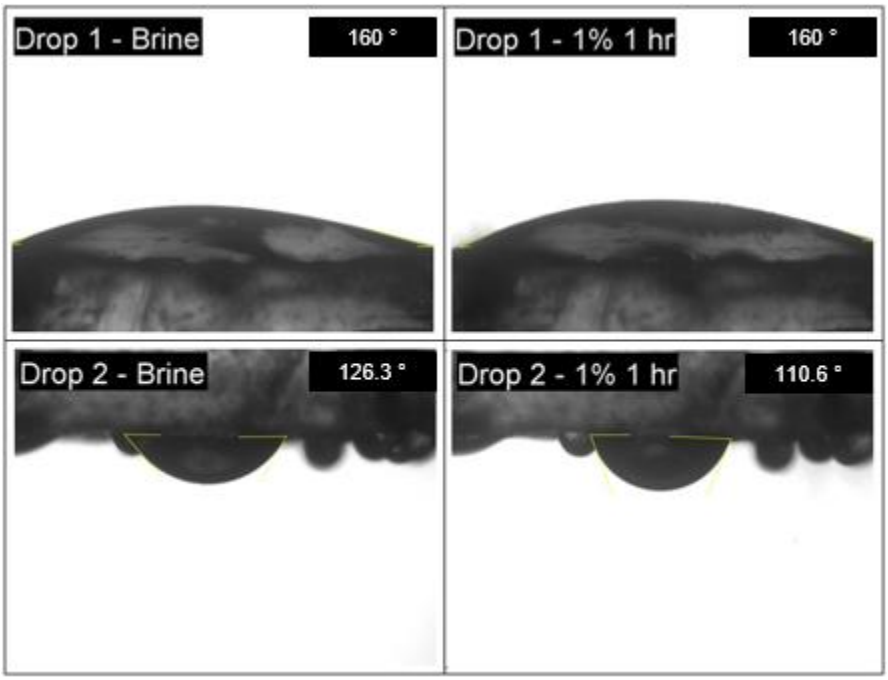

Figure 4-32: Contact angle changes with 1% UT Synthesized NX6+GLYMO

4.1.18 Wettability Experiments Summary

Tables 4-1 and 4-2 highlight the results of the wettability alteration experiments in terms of NP stability, final contact angle through the water phase (and change in contact angle). In all experiments prior to adding nanoparticles, the initial contact angles were above 90°.

Exp.	NP Solution	NP Stability (pH)	Final θ_c (-$\Delta\theta$)	Time	Remark
1	1% N 5 nm V-1	Instable (>8)	155.5 (0)	1 hr.	-
2	1% N 5 nm V-2	Foggy Layer (>8)	28-103 (23-152)	1.5 hr.	-
3	1% N 5 nm V-3.2	Foggy Layer (>8)	86.3 (31)	1 hr.	-
4	1% N 12 nm V-2	Foggy Layer (>8)	111.2-126.5 (7)	2 hr.	-
5	1% N 25 nm V-2	Foggy Layer (>8)	112-121 (4-25)	1 hr.	-
6-7	1% N 80 nm	Foggy Layer (>8)	N/A	Instant	OBST.
8	1% C X-100	Stable (>9)	164.8 (-55)	Instant	Snap off
9	1% C X-C	Stable (<3)	75 (38)	Instant	Snap off
10	1% C X-B	Unstable (<4)	N/A	Instant	-
11	1% C X-D	Stable (>9)	56 (65)	1 hr.	Snap off
12	1% NYACOL	Stable (<5)	117-125 (8-15)	4 hr.	-

Table 4-1: Summary of wettability experiments 1-12

Exp.	NP Solution	NP Stability (pH)	Final θ_c ($-\Delta\theta$)	Time	Remark
13	1% N 5 nm V-1	Stable (<6)	99.6 (41)	1 hr.	-
13	3% N 5 nm V-1	Stable (<6)	88.6 (52)	1 hr.	-
13	5% N 5 nm V-1	Stable (<6)	0 (141)	1 hr.	Snap off
14	1% N 5 nm V-2	Stable (<6)	118.6 (8)	1 hr.	-
14	3% N 5 nm V-2	Stable (<6)	67.4 (59)	1 hr.	-
14	5% N 5 nm V-2	Stable (<6)	131.4 (-5)	1 hr.	Snap off
15	1% N 5 nm V-3.2	Stable (<4)	103.2 (58)	1 hr.	-
15	3% N 5 nm V-3.2	Stable (<5)	0 (135)	Instant	Snap off
15	5% N 5 nm V-3.2	Stable (<6)	0 (135)	Instant	Snap off
16	1% C X-D	Stable (>9)	120.7 (16)	1 hr.	-
16	3% C X-D	Stable (>9)	0 (137)	Instant	Snap off
16	5% C X-D	Stable (>9)	0 (137)	Instant	Snap off
17	1% NX6+PEG	Stable (N/A)	97.3 (29)	3 hr.	Snap off
18	1% NX6+GLYMO	Stable (N/A)	111-160 (0-15)	1 hr.	-

Table 4-2: Summary of wettability experiments 13-18

In terms of contact angle change, two regimes are delineated, ones with stability issues and ones where they were resolved with pH control. In the case where pH was not controlled, the majority of Nissan nanoparticles did not change contact angles toward the water-wet range except with Nissan 5 nm V-2. The severity of aggregation with Nissan nanoparticles varied from total conglomeration to slight foggy layers appearing at the bottom of the cuvette. On the other hand, controlling pH resolved the stability issues of the Nissan nanoparticles where no signs of nanoparticles aggregation appeared. Moreover,

changes in contact angles toward an intermediate and oil-wet range observed with the three versions of the Nissan nanoparticles.

However, reducing pH seemed to weaken the effects of Nissan V-2 as the contact angle changed by only 8° at 1% concentration compared to more than 23° without reducing the system's pH. Nissan V-3.2 provided the greatest change in contact angle toward water wetness compared to the other Nissan versions after clearing the stability issue. Generally, increasing the concentration of Nissan nanoparticles changed the contact angle towards the water-wet range as indicated by the oil drop snap off at 3% or higher concentrations (the contact angle changes so drastically that the oil drop lifts off the surface).

NYACOL nanoparticles minimally changed the contact angle where the change did not exceed 15° in a period of 4 hours. Similarly, the in-house synthesized nanoparticles with GLYMO have the same minimal effect on contact angle as the NYACOL nanoparticles.

On the other hand, the synthesized nanoparticles with polyethylene glycol caused the contact angle to change towards an intermediate wetness range after snapping off a big portion of the original drop. Finally, Company X- C&D nanoparticles changed the contact angle towards a water-wet range. Company X-100 snapped off a big portion of the original drop while the remaining portion had a strong oil-wet contact angle.

4.2 Interfacial Tension Alteration Experiments

The pendent drop method was used to perform 12 interfacial tension change experiments between brine and oil at the presence of various nanoparticle solutions. The used nanoparticles solution samples were provided by Nissan, NYACOL, and Company X. Two more samples were synthesized at the University of Texas at Austin and were used

in the last two experiments. Brine with 8% NaCl was used in all of the experiments in this section.

The interfacial tension was measured between oil and brine before injecting nanoparticles to establish a comparison control base. The brine-oil IFT was measured at three different nanoparticles concentrations, 1%, 3%, and 5%. Measurements of IFT are recorded at time interval of 3 minutes for a period of 30 minutes or more at every nanoparticles concentration in all experiments.

4.2.1 Experiment 1: 1%, 3% and 5% Nissan 5 nm V-1

The control IFT in this experiment was calculated to be 26.90 dynes/cm. The hanging drop on the inverted needle is shown on Figure 4-33 for the control case. As shown on Figure 4-34, the reduction in IFT with time was highest in the case with 1% nanoparticles and lowest in the case with 5% nanoparticles. Generally, the reduction in IFT between brine and oil in the presence of nanoparticles was insignificant with a lowest measured value of 21.22 dynes/cm at the end of one hour period. The increase in nanoparticles concentration decelerated IFT reduction with time. The pH of the solution was reduced to values below 6 using amounts of less than 0.5 ml diluted HCl at every nanoparticles concentration to ensure particles stability.

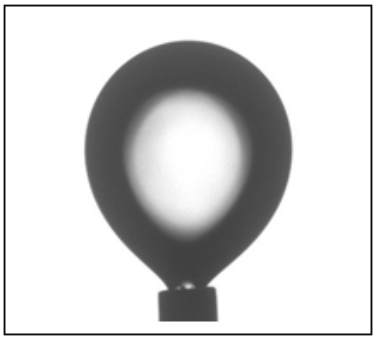

Figure 4-33: Control case hanging oil drop on the inverted needle

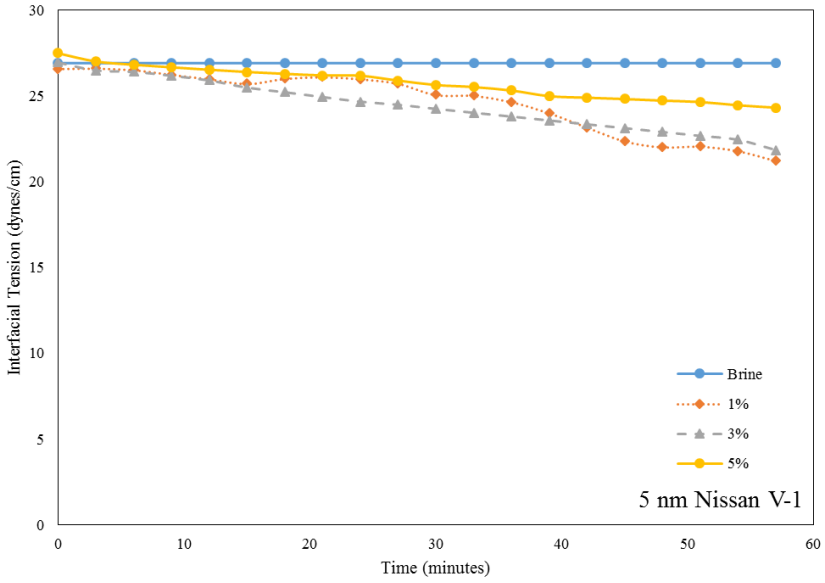

Figure 4-34: Oil/Brine IFT changes with Nissan 5 nm V-1 nanoparticles

4.2.2 Experiment 2: 1%, 3% and 5% Nissan 5 nm V-2

The control case IFT was 28.40 dynes/cm. For a period of 39 minutes, the reduction in IFT seems to be the greatest using a 1% nanoparticles concentration; however, from the beginning of the experiment until 30 minutes later, the 3% concentration provided the lowest IFT values, see Figure 4-35. The nanoparticles did not seem to significantly reduce IFT with 23.47 dynes/cm being the lowest IFT reached at 1% concentration. Moreover, the IFT values for all concentrations plateaued from time zero except for the 1% concentration after 30 minutes. The pH of the solution was reduced to values below 6 using amounts of less than 0.5 ml diluted HCl at every nanoparticles concentration to ensure particles stability.

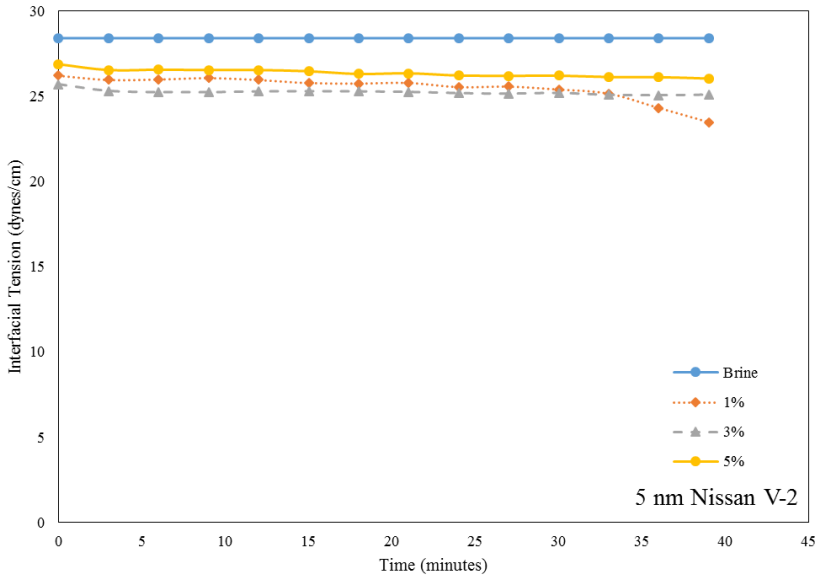

Figure 4-35: Oil/Brine IFT changes with Nissan 5 nm V-2 nanoparticles

4.2.3 Experiment 3: 1%, 3% and 5% Nissan 5 nm V-3.2

Adding 1% nanoparticles concentration to the brine solution increased the oil/brine IFT slightly from 28.40 dynes/cm to 31.88 dynes/cm. Moreover, the IFT decreased with time until it approached the control case IFT value after 33 minutes. The increase in nanoparticles concentration seems to further reduce IFT but the change with time is negligible, see Figure 4-36. Similar to the previous two experiments, the reduction in IFT is insignificant with the lowest measured IFT being 24.55 dynes/cm at 5% nanoparticles concentration. The pH of the solution was reduced to values below 6 using amounts of less than 0.5 ml diluted HCl at every nanoparticles concentration to ensure particles stability.

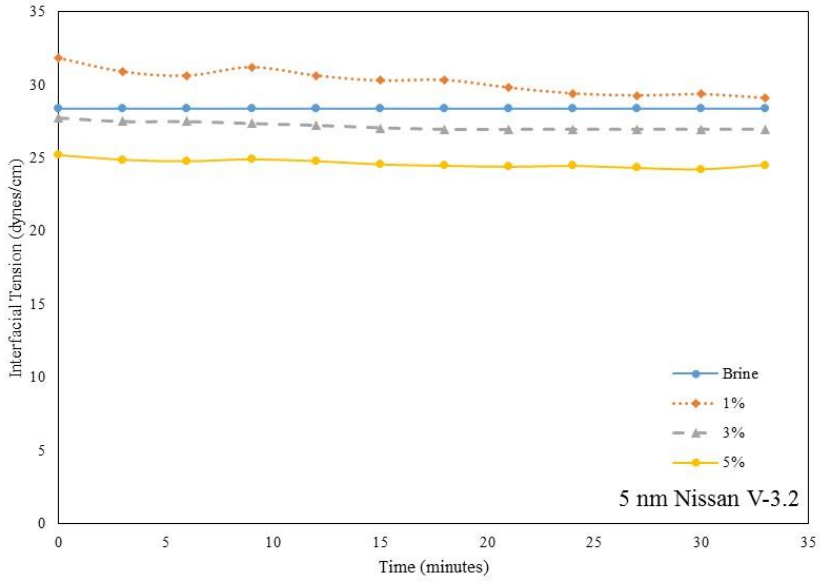

Figure 4-36: Oil/Brine IFT changes with Nissan 5 nm V-3.2 nanoparticles

4.2.4 Experiment 4: 1%, 3% and 5% Nissan 12 nm V-2

The control case IFT is 28.40 dynes/cm. A slight increase of oil/brine IFT has been observed when adding 1% of the Nissan 12 nm V-2 nanoparticles, which reduces back to the control case IFT after a period of 30 minutes. The increase in nanoparticles concentration have generally reduced IFT below the control case IFT value, but the reduction is insignificant. The lowest measured IFT is 24 dynes/cm at 5% nanoparticles concentration, see Figure 4-37. The pH of the solution was reduced to values below 6 using amounts of less than 0.5 ml diluted HCl at every nanoparticles concentration to ensure particles stability.

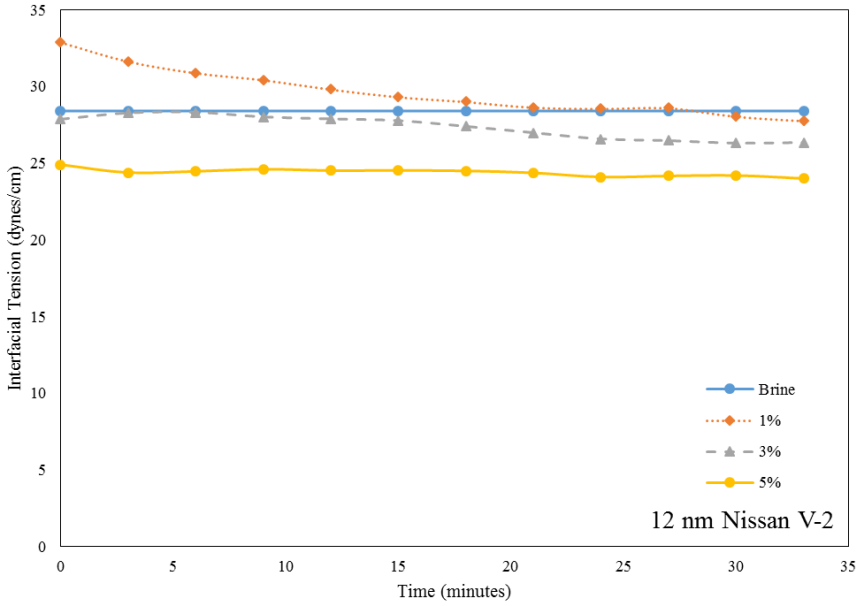

Figure 4-37: Oil/Brine IFT changes with Nissan 12 nm V-2 nanoparticles

4.2.5 Experiment 5: 1%, 3% and 5% NYACOL 46 nm

The addition of the nanoparticles to the brine solution have negligibly reduced IFT over time. In fact, at 1% and 3% nanoparticles concentration, IFT increased slightly above the control case. A trivial reduction in IFT with time have started to appear after increasing the particles concentration to 5%, see Figure 4-38. No pH reduction was necessary in this experiment as the stock nanoparticles concentration was acidic and the pH values were below 4 at all nanoparticles concentrations. The solution was clear with no signs of particles aggregation.

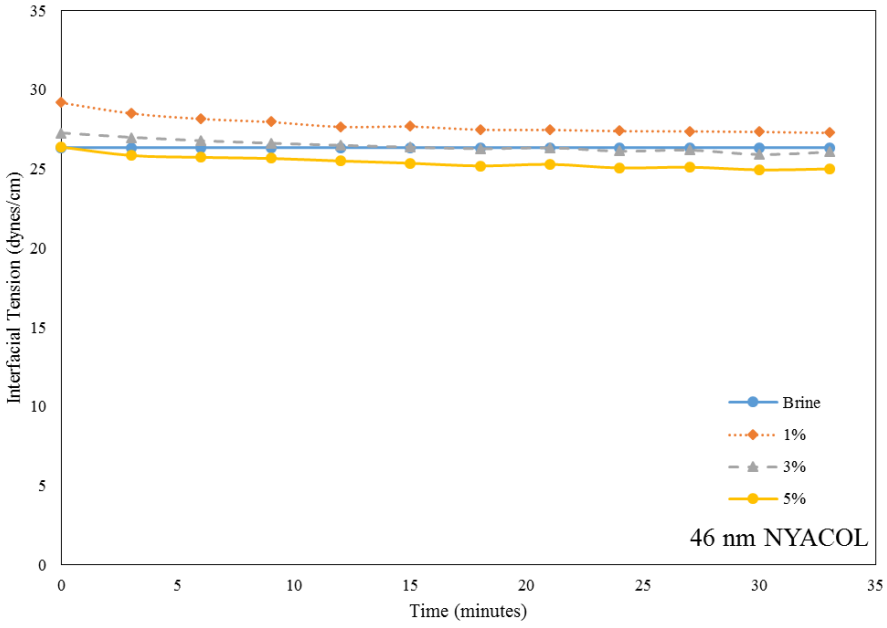

Figure 4-38: Oil/Brine IFT changes with NYACOL 46 nm nanoparticles

4.2.6 Experiment 6: 1%, 3% and 5% Nissan 25 nm V-2

The IFT increased above the control case IFT with 1% and 3% nanoparticles concentrations. Within a 30 minutes period, the IFT reduced to and slightly lower than the control case IFT for the 1% concentration case; however, IFT remained higher than the control case for the 3% concentration case. For the 5% particles concentration, the IFT started at the control case IFT and reduced to a plateau IFT value of 23 dynes/cm after 25 minutes, see Figure 4-39. Generally, the change in IFT is insignificant. The pH of the solution was reduced to values below 6 using amounts of less than 0.5 ml diluted HCl at every nanoparticles concentration to ensure particles stability.

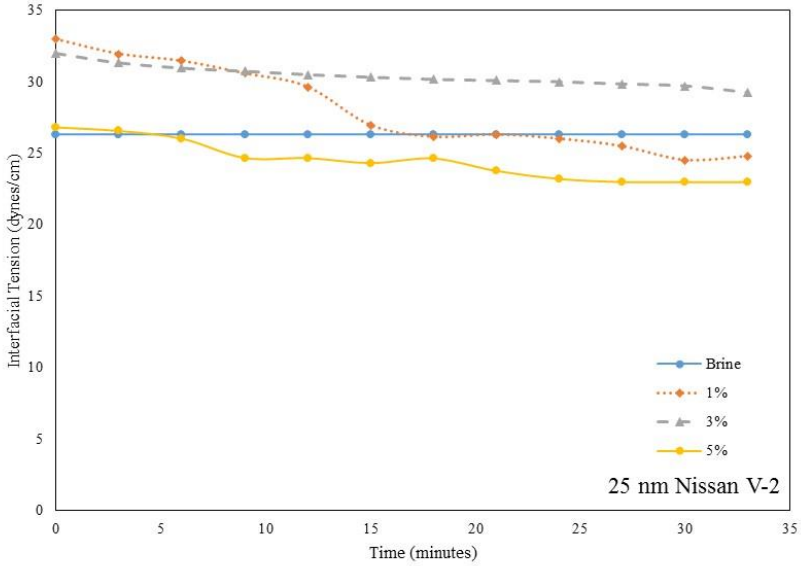

Figure 4-39: Oil/Brine IFT changes with Nissan 25 nm V-2 nanoparticles

4.2.7 Experiment 7: 1%, 3% and 5% 5 nm Company X-100

The control case IFT is 25.65 dynes/cm. Adding 1% nanoparticles concentration to the brine solution have reduced IFT significantly to 6.66 dynes/cm as shown in Figure 4-40. The change of IFT with time was minimal with the lowest IFT of 5.59 dynes/cm after 30 minutes. Furthermore, increasing nanoparticles concentration reduced IFT down to 1.17 dynes/cm at 3% concentration and 0.46 dynes/cm at 5% concentration. Change of IFT with time measurements at 3-5% concentrations was not possible as the hanging drop on the inverted needle snaps off after one or two IFT measurements. Figure 4-41 shows the small hanging drop size on the inverted needle in this experiment. Reducing pH of the solution was not necessary as the nanoparticles were stable and no signs of aggregation appeared.

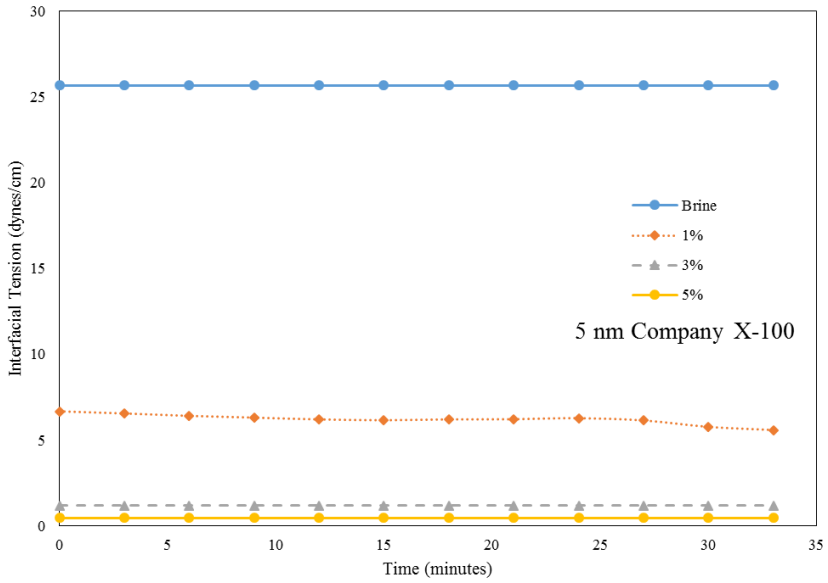

Figure 4-40: Oil/Brine IFT changes with 5 nm Company X-100 nanoparticles

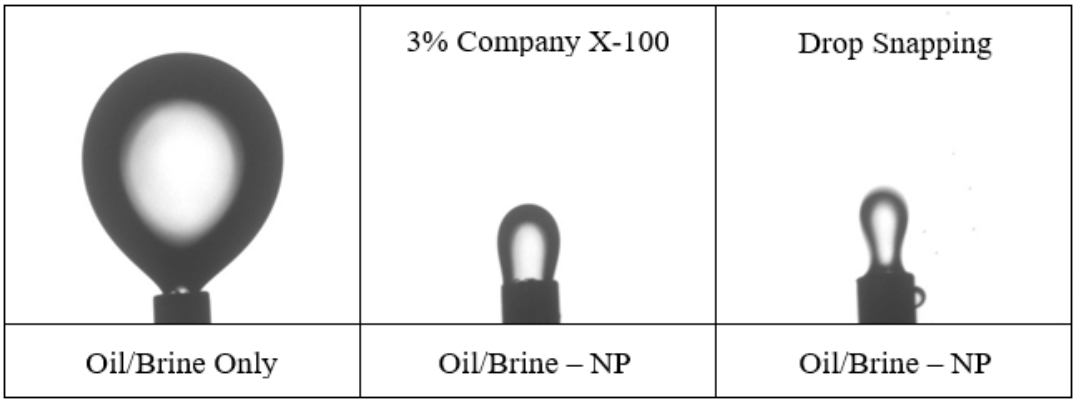

Figure 4-41: Hanging drop size comparison between control and Company X NP cases

4.2.8 Experiment 8: 1%, 3% and 5% 5 nm Company X-B

The control case IFT was 27.33 dynes/cm. At 1% nanoparticles concentration, IFT value reduced to 10 dynes/cm initially and it kept reducing until a cut of 50% IFT value reached after 9 minutes, see Figure 4-42. Moreover, increasing the particles concentration have further reduced IFT significantly down to 1.94 dynes/cm and 0.47 dynes/cm at 3%

and 5% concentrations, respectively. At the latter concentrations, IFT measurements with time were not possible as the hanging drop on the inverted needle snaps off after one or two IFT measurements. Reducing pH of the solution was not necessary as the nanoparticles were stable and no signs of aggregation appeared.

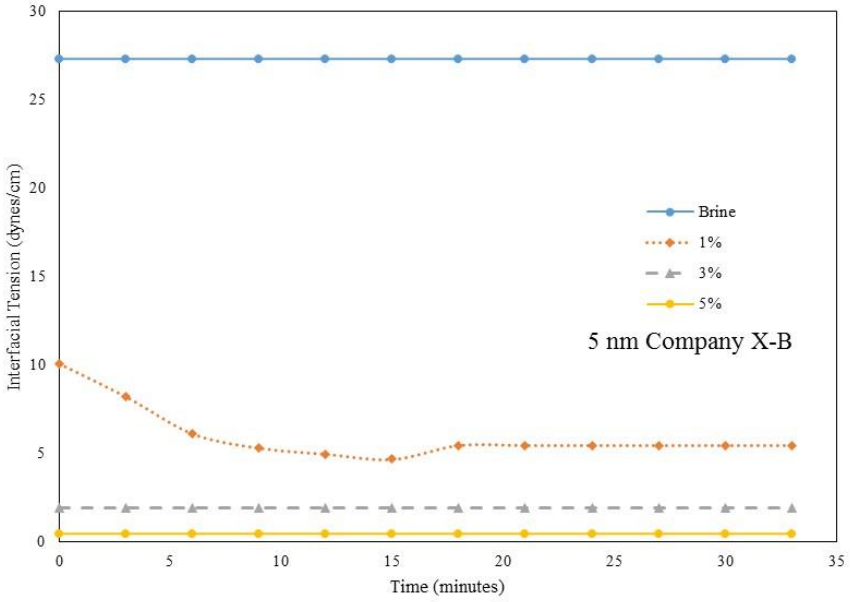

Figure 4-42: Oil/Brine IFT changes with 5 nm Company X-B nanoparticles

4.2.9 Experiment 9: 1%, 3% and 5% 5 nm Company X-C

The control case IFT was 26.05 dynes/cm. Adding 1% of the Company X-C nanoparticles in the brine solution have significantly reduced IFT to 8.23 dynes/cm. Within a period of approximately 20 minutes, IFT reduced down to 4.92 dynes/cm which plateaued at 3.36 dynes/cm after 30 minutes. Additionally, the increase in nanoparticles concentration reduces IFT more as shown in Figure 4-43. The IFT values reduced down to 0.92 dynes/cm and 0.45 dynes/cm at 3% and 5% nanoparticles concentrations, respectively. Similar to the previous two experiments, it was not possible to measure IFT change with time for

concentrations above 1% as the hanging drop keeps snapping off. Reducing pH of the solution was not necessary as the nanoparticles were stable and no signs of aggregation appeared.

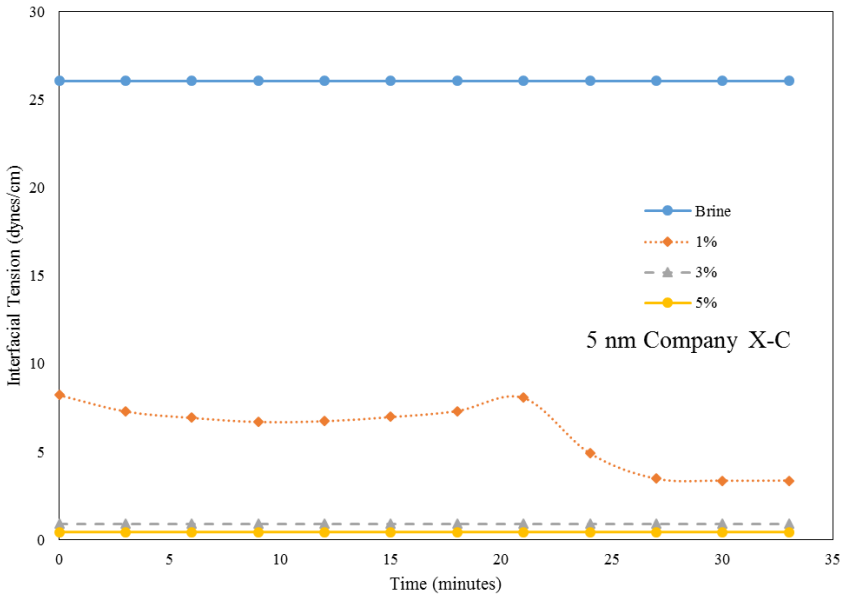

Figure 4-43: Oil/Brine IFT changes with 5 nm Company X-C nanoparticles

4.2.10 Experiment 10: 1%, 3% and 5% 5 nm Company X-D

Adding 1% of the nanoparticles significantly reduced IFT down to 6.54 dynes/cm. In a period of 25 minutes, the IFT plateaued at 4.56 dynes/cm which indicates a slow decreases over time as shown in Figure 4-44. The increase in nanoparticles concentration further reduced IFT to small values of 1.22 dynes/cm and 0.75 dynes/cm at 3% and 5% concentrations, respectively. Measuring IFT with time was not possible for 3-5% concentrations as the hanging drop on the inverted needle snapped off after one or two IFT measurements. Reducing pH of the solution was not necessary as the nanoparticles were stable and no signs of aggregation appeared.

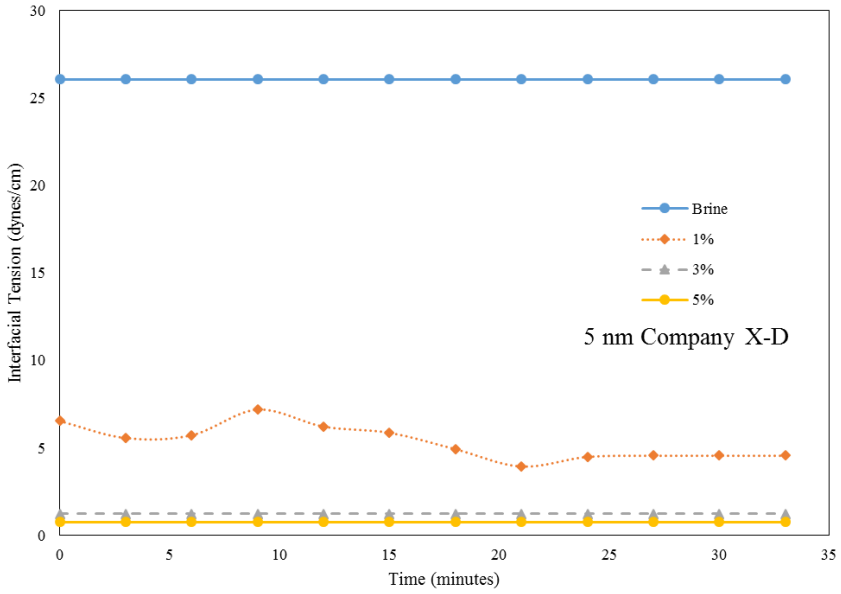

Figure 4-44: Oil/Brine IFT changes with 5 nm Company X-D nanoparticles

4.2.11 Experiment 11: 1%, 3% and 5% UT Synthesized NX6+PEG (6-9 EO)

The nanoparticles sample used here was synthesized at the University of Texas at Austin as mentioned and explained in experiment 17 in the wettability alteration section of this chapter. The measured control case IFT was 25.20 dynes/cm. The addition of 1% of the nanoparticles caused an instant reduction in IFT to 18.10 dynes/cm. Moreover, IFT kept reducing slowly with time until it plateaued at 15.30 dynes/cm after 30 minutes. In addition, it is clear from the IFT with time data on Figure 4-45 that the increase in nanoparticles concentration causes higher reduction in IFT values. After 25 minutes, IFT values plateaued at 11.22 dynes/cm and 8.59 dynes/cm for 3% and 5% concentrations, respectively. Reducing pH of the solution was not necessary as the nanoparticles were stable and no signs of aggregation appeared.

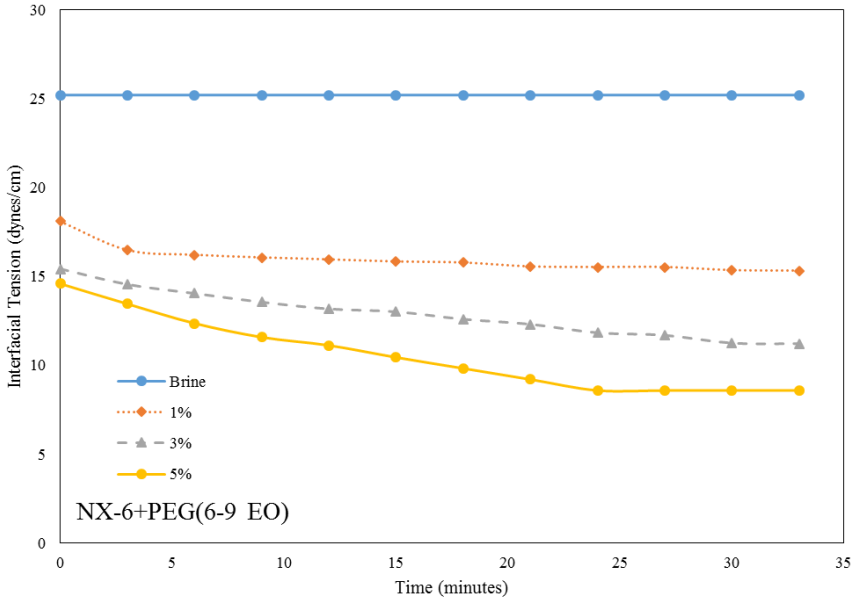

Figure 4-45: Oil/Brine IFT changes with UT Synthesized NX6+PEG (6-9 EO)

4.2.12 Experiment 12: 1%, 3% and 5% UT Synthesized NX6+GLYMO

The control case IFT was 25.20 dynes/cm. The increase of the nanoparticles concentration to 1% in the brine solution caused the IFT to drop to 21.45 dynes/cm which remained consistent around this value for all of the testing 33 minutes period. Moreover, increasing the concentration to 3% has further reduced IFT down to approximately 17 dynes/cm; however, the additional increase in nanoparticles concentration did not seem to reduce IFT more as in the case with 5% concentration, see Figure 4-46. Reducing pH of the solution was not necessary as the nanoparticles were stable and no signs of aggregation appeared.

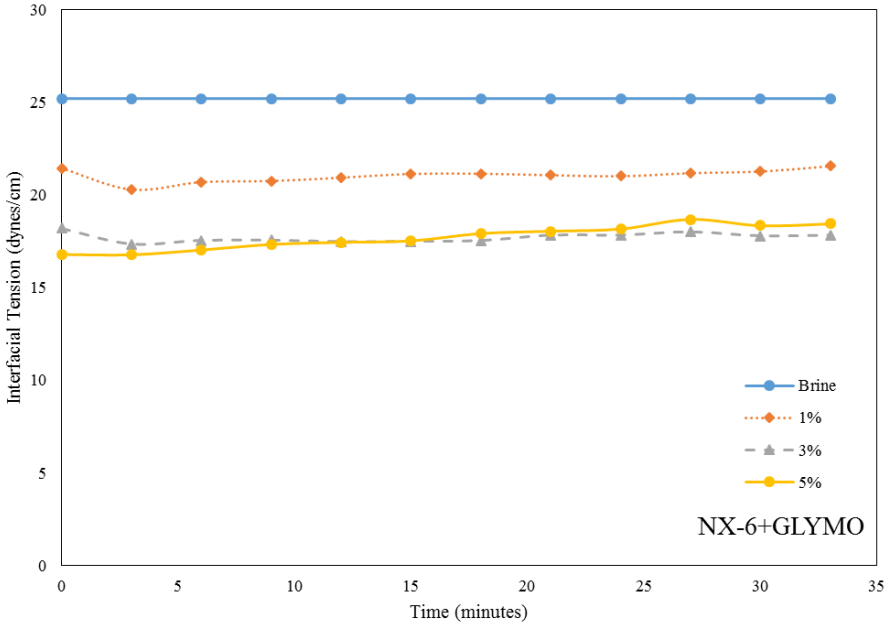

Figure 4-46: Oil/Brine IFT changes with UT Synthesized NX6+ GLYMO

4.2.13 Interfacial Tension Experiments Summary

Table 4-3 summarizes the achieved oil/brine IFT values by all the tested solutions. Only sodium chloride brine was used in all experiments. The table shows the percent change in IFT by each nanoparticles sample. Nissan and NYACOL nanoparticles did not effectively reduce IFT where the reduction ranged from 0% to 8%. In fact, two samples from Nissan, 5 nm V-3.2 and 12 nm V-2, have increased the value of IFT by 5.8% and 8%, respectively. On the other hand, the in-house synthesized nanoparticles with GLYMO have reduced IFT by a factor of 25%. The in-house synthesized nanoparticles with polyethylene glycol have reduced IFT down to 15.97 dynes/cm which represent 43% of change.

The biggest change in IFT was achieved using Company X nanoparticles where a reduction of more than 77% of the original IFT occurred. It is worth noting that Company X-D, which has the highest polyethylene glycol coverage on the nanoparticles surface, reduced the IFT down to 5.35 dynes/cm which represents more than 80% of IFT reduction.

As depicted on Figure 4-47, the increase in nanoparticles concentration supports the higher reduction in IFT by all nanoparticle solution samples.

Exp. No.	Solution	Average IFT, dynes/cm	Change Percentage
Control	Brine	28.00	0.00
1	1% 5 nm Nissan V-1	25.96	-7.30
2	1% 5 nm Nissan V-2	25.76	-8.02
3	1% 5 nm Nissan V-3.2	30.26	8.08
4	1% 12 nm Nissan V-2	29.63	5.83
5	1% 25 nm Nissan V-2	28.09	0.31
6	1% 46 nm NYACOL	27.80	-0.73
7	1% 5 nm Company X-100	6.20	-77.85
8	1% 5 nm Company X-B	6.02	-78.50
9	1% 5 nm Company X-C	6.12	-78.16
10	1% 5 nm Company X-D	5.35	-80.90
11	1% NX-6+PEG(6-9 EO)	15.97	-42.96
12	1% NX-6+GLYMO	21.04	-24.86

Table 4-3: Summery of IFT experiments 1-12

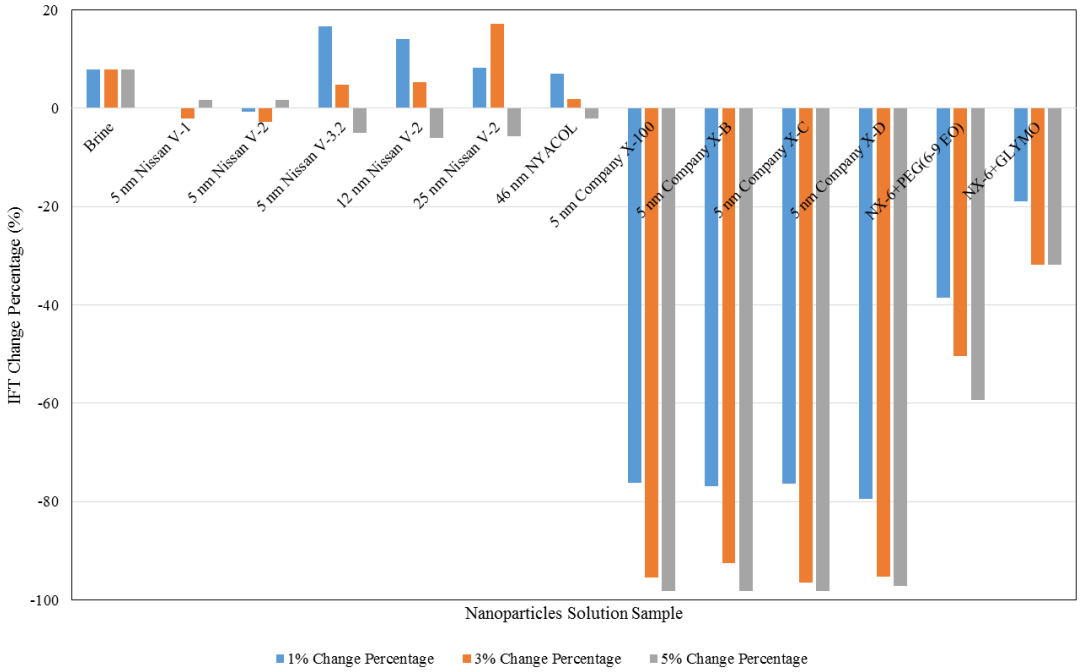

Figure 4-47: Percent change of IFT at 1%, 3% and 5% nanoparticles concentrations

4.3 Nanoparticles Stability Test At High Salinity and Low pH

The synthesized nanoparticles at the university and the samples from Company X were not experimented on under low pH conditions as they proved being stable under high pH values and high salinities except for Company X-B sample which lost stability under low pH conditions. The testing solution for all samples contained 8% NaCl, 3% nanoparticles, and HCl to reduce pH. As shown in Figure 4-48 and Figure 4-49, all samples sustained stability at this high salinity and pH values less than 5 for more than 24 hours except for Company X-B nanoparticles which lost stability immediately after reducing pH. It is clear from the white layer in the glass container that the nanoparticles have aggregated immediately and settled down after 24 hours. It is important to know that a certain nanoparticles solution will remain stable at low pH conditions especially when working with CO_2 applications as the medium becomes more acidic.

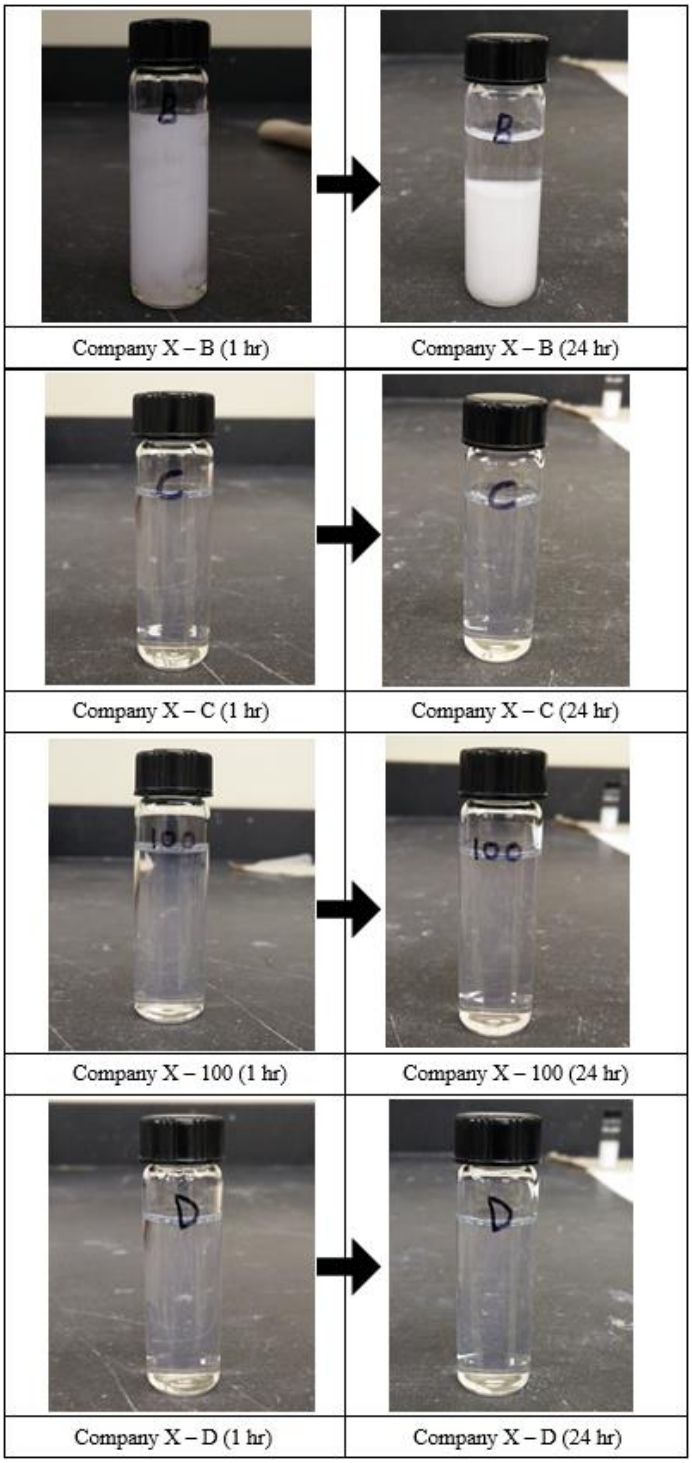

Figure 4-48: Company X nanoparticles stability test at high salinity and low pH

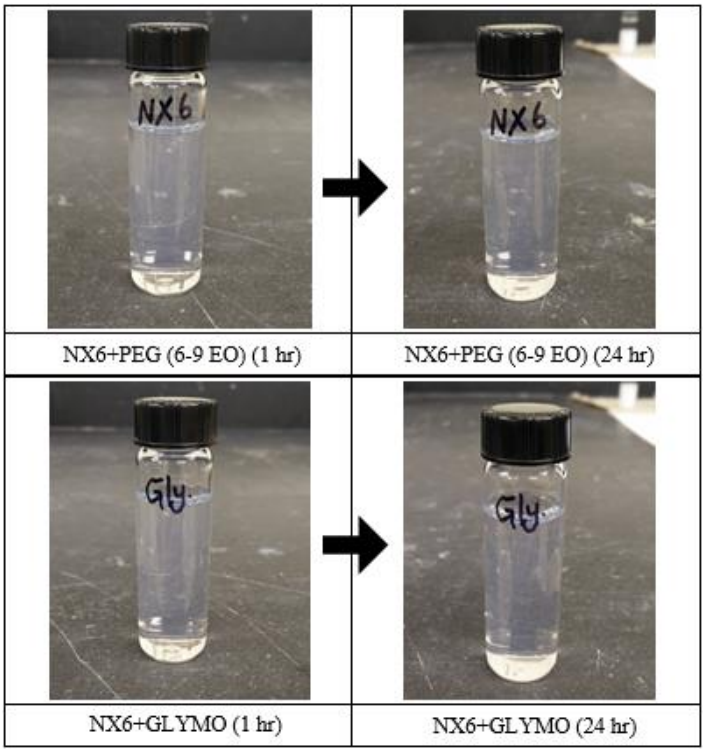

Figure 4-49: UT synthesized nanoparticles stability test at high salinity and low pH

4.4 Oil Drop Behavior In Nanoparticle Solution Experiment

Figure 4-50 shows oil drops and patches infused in a brine solution with nanoparticles and the drops are maintaining the spherical shape without coalescing with nearby drops as nanoparticles are surrounding them. Similarly, multiple oil patches are not coalescing due to the presence of nanoparticles that are potentially masking them. Normally, oil drops or patches will merge and form one single layer on top of the water as oil has lower density. Nissan V-1 and the in-house synthesized nanoparticles with polyethylene glycol were used in this experiment. Nissan nanoparticles produced spherical oil droplets that have a maximum diameter of 3.33 mm. In contrast, the synthesized nanoparticles with PEG produced circular oil patches on top of the water surface. These oil sections did not spread or coalesce.

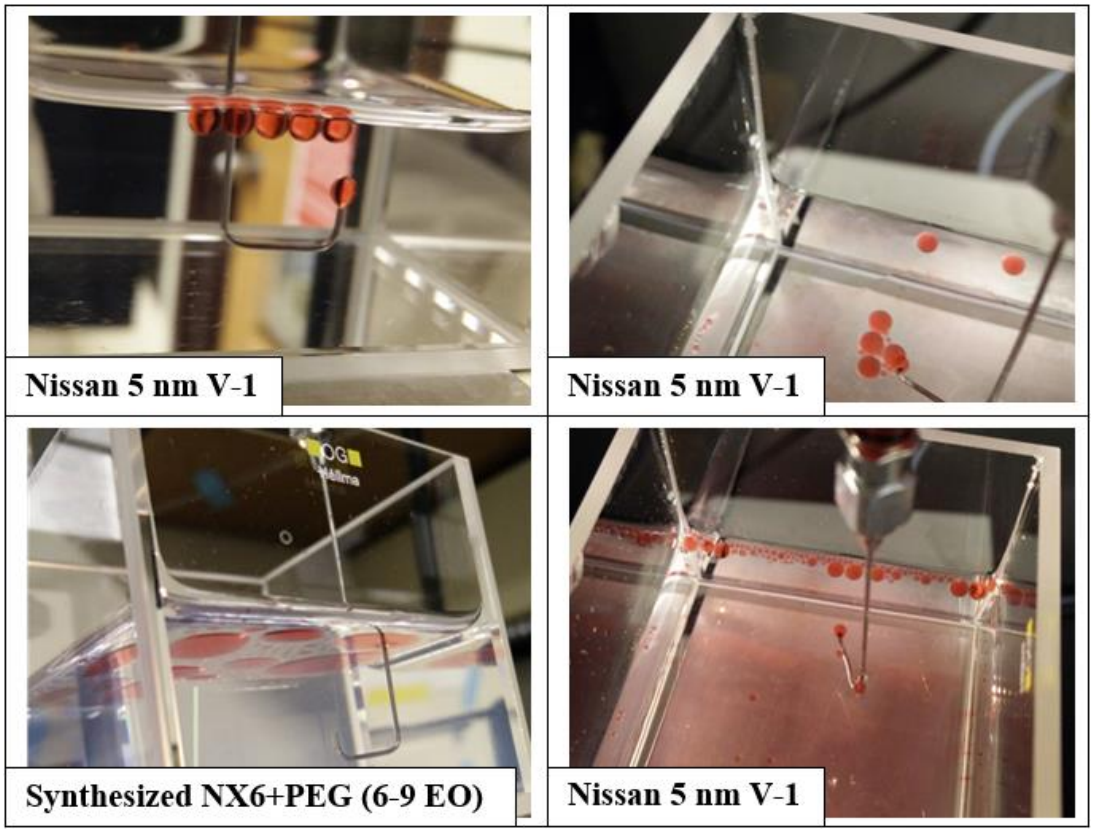

Figure 4-50: Oil drops and patches not spreading or coalescing due to the presence of nanoparticles

4.5 Discussion of the Results

This section covers a discussion of the results from the wettability and IFT experiments.

4.5.1 IFT Results Comparison

The results of the IFT change experiments were inconsistent upon introducing different nanoparticle solutions to the brine and oil system. The variation includes values of IFT higher than the control case (brine/oil) IFT and values that are significantly lower than the control case IFT.

4.5.1.1 Nissan Nanoparticles Versions

The three tested versions from Nissan have different chemical mixtures and nanoparticles coating. Nissan nanoparticles are grafted with ethylene glycol and the different versions have different coverage percentages on the nanoparticles which are not specifically disclosed. Moreover, polyethylene glycol is included in the currying solution with the water instead of the nanoparticles' surface. Despite the insignificant change in IFT with Nissan nanoparticles, versions 1 and 2 seem to be on the lower side of IFT values as shown in Figure 4-51. On the other hand, version 3.2 seems to increase the IFT slightly above the control case unless the concentration of nanoparticles is higher than 1% as shown in the respective version 3.2 IFT experiment.

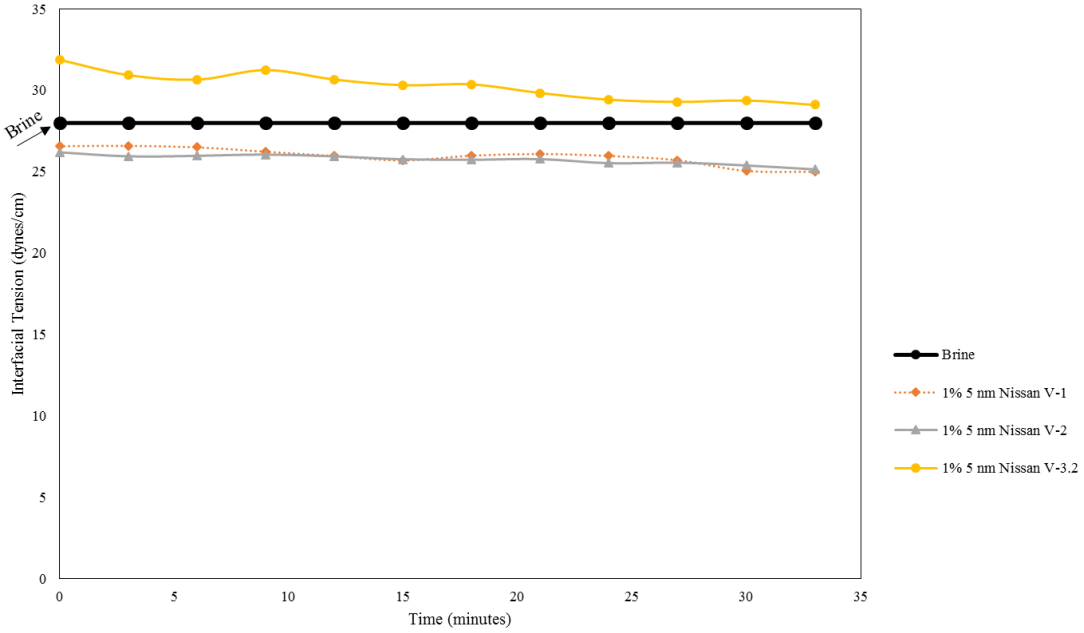

Figure 4-51: IFT change - Nissan nanoparticles different versions comparison

4.5.1.2 Nanoparticles Size Effects

Nissan provided version 2 nanoparticle solutions with different nanoparticles sizes ranging from 5 to 25 nm which allows the analysis of the effects of nanoparticles size on

IFT change. As shown in Figure 4-52, the nanoparticles with the smallest diameter reduced IFT the most. However, the reduction in IFT was not consistent with the size of the nanoparticles as the highest diameter particles started at the highest IFT value but reduced to IFT values comparable to the particles with the 5 nm diameter after 15 minutes. This comparison indicates that higher nanoparticles sizes might slow the rate of desirable IFT reduction.

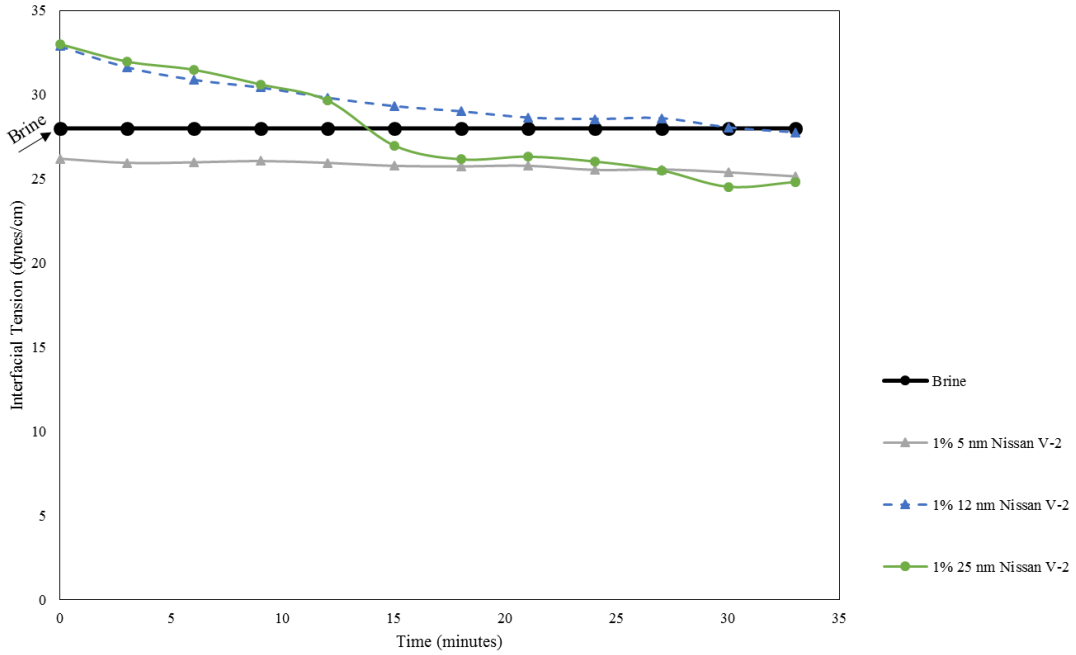

Figure 4-52: IFT change - Nissan V-2 nanoparticles different size comparison

4.5.1.3 Company X Nanoparticles Versions (Coating Percentage Effect)

Company X (not the actual name) provided four samples that have nanoparticles grafted with polyethylene glycol at different coverage percentages. Moreover, the particles' carrying solution contents are not disclosed due to the company's confidentiality measures. The particles coating percentage is highest with version D and lowest with version B with version 100 being in between C and D. All of the samples here reduced IFT

significantly at 1% nanoparticles concentration, see Figure 4-53. In addition, it is clear that higher nanoparticles coating percentages causes higher reduction in IFT, especially at the first five minutes of nanoparticles exposure. At the later period, the IFT values fluctuate and overlap but with an overall decreasing trend.

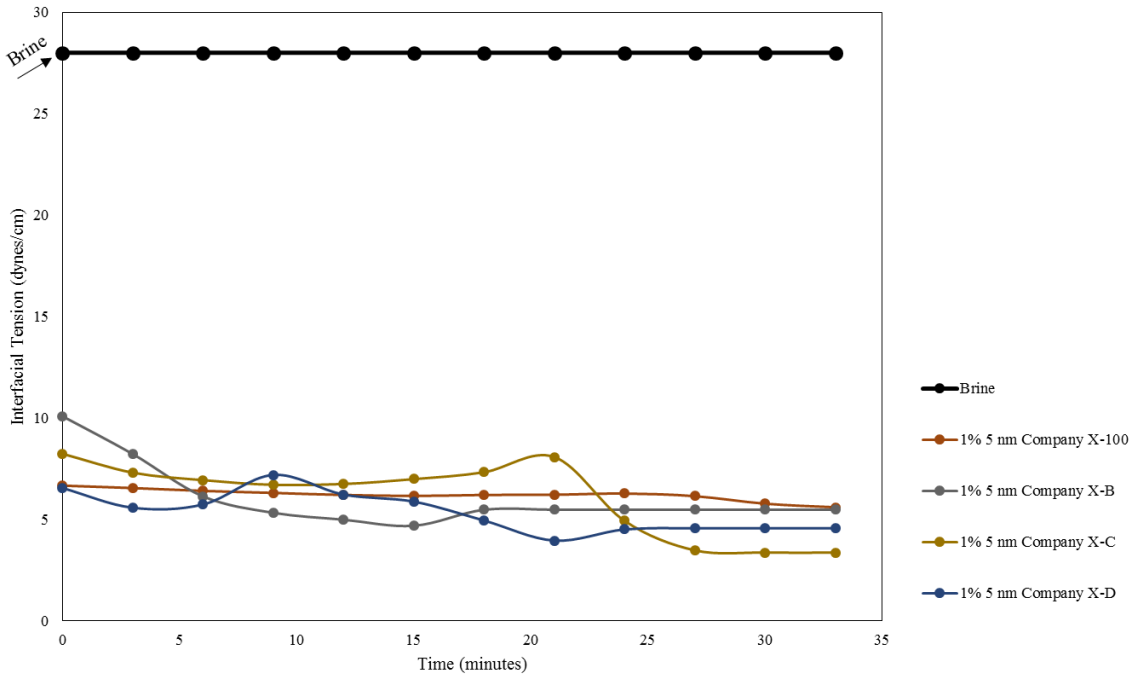

Figure 4-53: IFT change – Company X nanoparticles different versions comparison

4.5.1.4 In-House Synthesized Nanoparticle Solutions

Both solutions showed a degree of IFT reduction as shown in Figure 4-54. The reduction trends of both solution were not similar where the nanoparticles coated with GLYMO resulted in IFTs higher than 20 dynes/cm and did not reduce with time. Conversely, the nanoparticles coated with polyethylene glycol resulted in a lower IFT value that decreased with time until it reached approximately 15 dynes/cm. The polyethylene glycol seems to affect IFT more than the GLYMO.

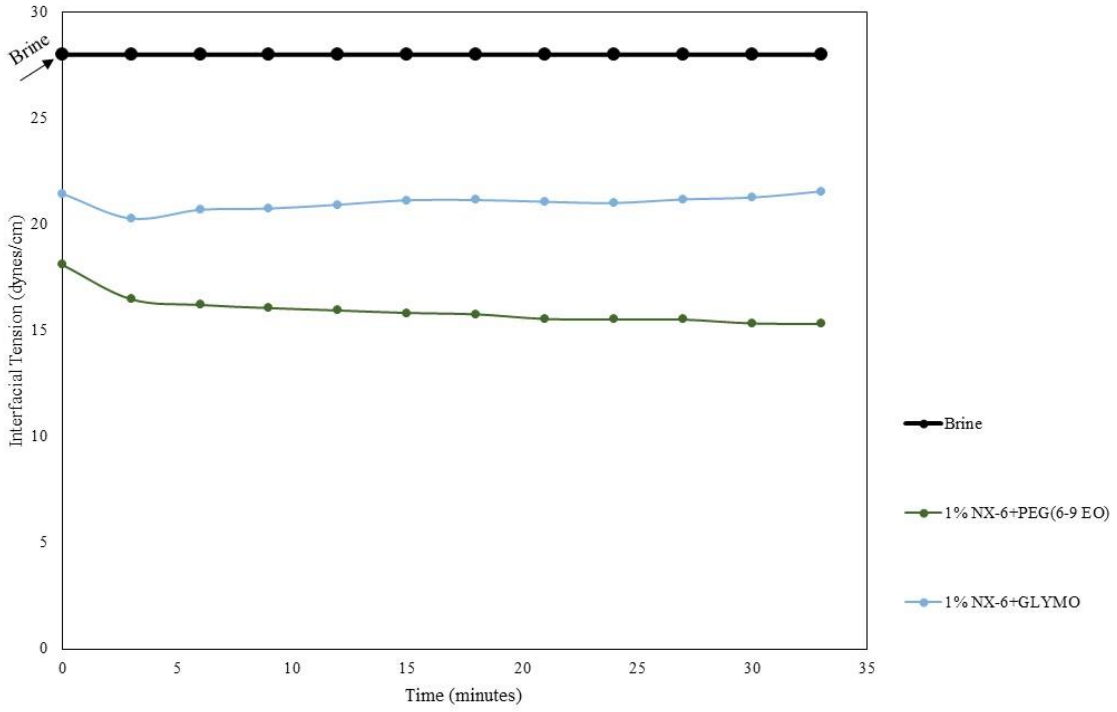

Figure 4-54: IFT change – in-house synthesized nanoparticles comparison

4.5.1.5 All Samples Comparison

The change in IFT was different using the various nanoparticle solutions in this study as depicted in Figure 4-55. Moreover, Figure 4-56 presents the average IFT change percentage at 1% nanoparticles concentration. The highest reduction in IFT was achieved by Company X's samples followed by the solutions synthesized in-house where the IFT change percentages reached -80% and -43%, respectively. On the other hand, the lowest change in IFT was noticed to be from Nissan and NYACOL solutions. Traces of surfactants are suspected to be in the nanoparticles carrying fluids of the Company X's samples, which explains the high reduction in IFT. Moreover, gaining more knowledge about the chain length of the polyethylene glycol used in the solution or for coating the nanoparticles would help create better comparison means to design the desired nanoparticles solution.

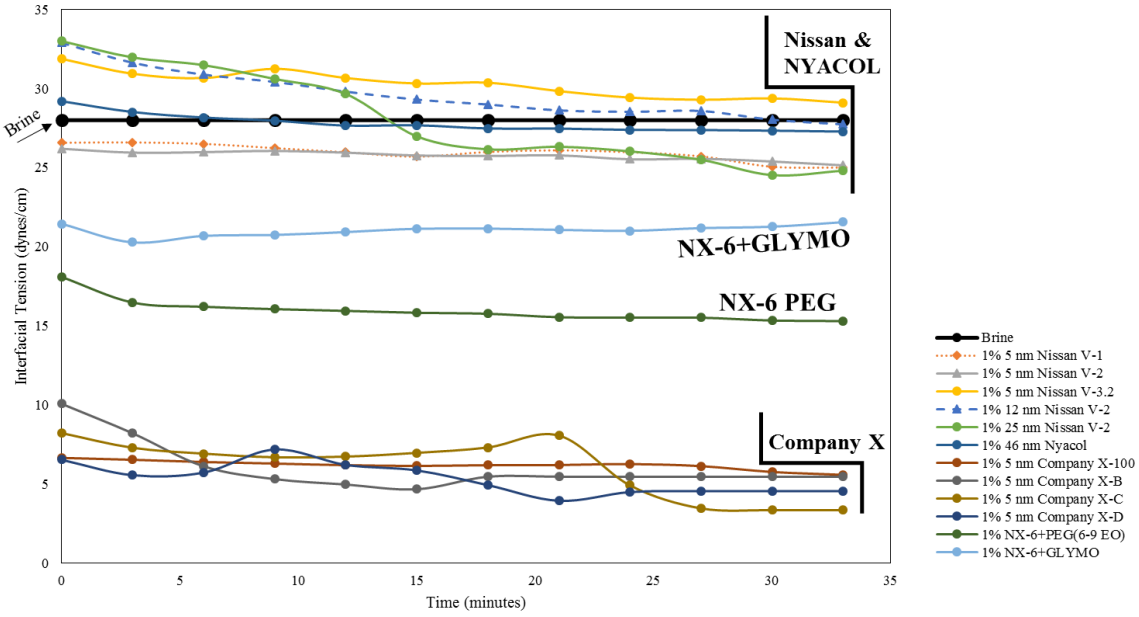

Figure 4-55: Comparison of IFT change from all used nanoparticles samples

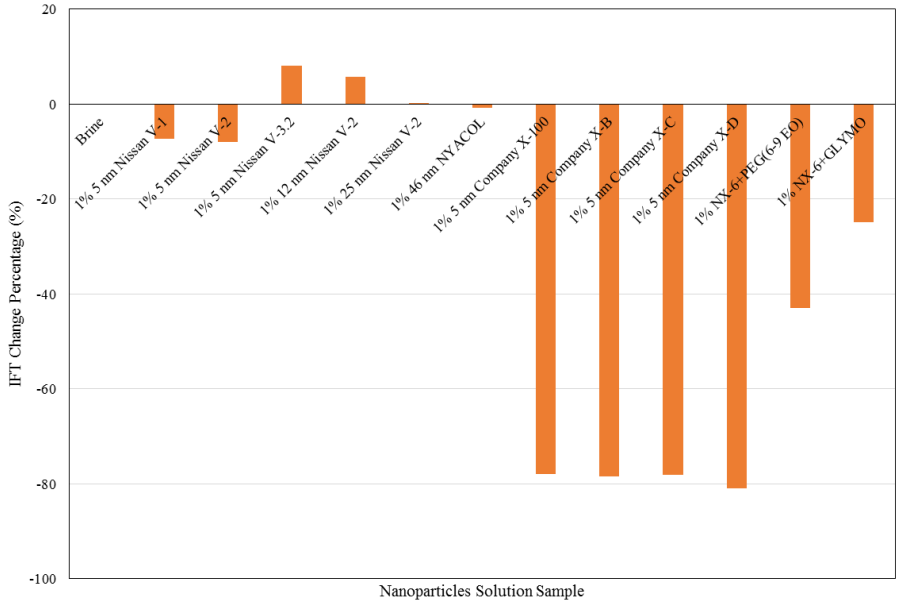

Figure 4-56: Percent change of IFT for every used nanoparticles sample

4.5.2 Wettability and IFT Alteration Results

The results of the wettability and IFT experiments done in this study indicate that the nanoparticle solutions may or may not alter the wettability on the carbonate surface and the brine/oil IFT, refer to the summary tables 4-1, 4-2 and 4-3. The results indicate that nanoparticles may change wettability if they are stable where they are suspended in solution. Nissan nanoparticles required pH control where HCl was added to achieve pH values below 6. Company X, NYACOL and the in-house synthesized nanoparticles were stable and did not require any pH control to remain suspended in solution.

Prior to reducing the solution's pH, Nissan nanoparticles did not alter the carbonate surface wettability except in small spots of the carbonate surface in experiment 2 when Nissan 5 nm V-2 sample was used. Resolving the particle stability issue by reducing the solution's pH resulted in increased changes of contact angle for the Nissan NPs, with the nanoparticle solutions were able to change the surface wettability to an intermediate wetness range at 1% nanoparticles concentration as shown in experiments 13, 14 and 15 (contact angles from 80° to 100°).

Increasing Nissan NPs concentration caused some of the oil droplets to snap off. Nissan nanoparticle solutions vary their formulations by adding polyethylene glycol to the carrying solution and by changing the particles surface coverage with ethylene glycol. No more details were revealed about the chemical content. No general trend was observed about the severity of wettability alteration, but Nissan V-3.2 seemed to obtain the biggest effect on wettability after resolving the stability issue. Nissan nanoparticles showed minimal changes in IFT.

On the other hand, samples from Company X showed moderate to high changes (down to 56° contact angle) in contact angle on the calcite surface. Some oil droplets snapped off the calcite surface at 1% NPs concentration. Increasing the concentration

caused more oil droplets to snap off. All Company X NPs are grafted with polyethylene glycol with version A having the lowest particle surface coverage and version D having the highest particle surface coverage. No details about the carrying solution were disclosed. It was observed that the higher the particle surface coverage, the higher the change on contact angle. Company X nanoparticles showed a great impact on IFT with values being reduced to 6 dynes/cm or below at 1% NPs concentration. Increasing NPs concentration caused IFT to reduce to values below 1 dyne/cm.

In contrast, the sample from NYACOL showed no change in contact angle on the calcite plate surface. No details about the formulation were disclosed. It is worth mentioning that the NYACOL used sample was acidic and the solution's pH reduced to 4.75 after adding the nanoparticles. NYACOL sample showed little or no changes in IFT.

Similarly, in-house synthesized nanoparticles with GLYMO showed no change in contact angle on the calcite plate surface. However, it showed moderate changes in IFT as it lowered IFT value to 21 dynes/cm. Finally, synthesized NPs with polyethylene glycol showed moderate change in contact angle (~98°). They also showed a moderate reduction in IFT with values that decreased to 16 dynes/cm.

Multiple drops in experiments 8 through 11 and experiment 17 have snapped totally off the calcite surface, wedged off where only a small portion of the drop remained, and reduced contact angle towards the water-wet range after contacting the injected nanoparticles.

4.5.2.1 Interpretation of Results

The results are interpreted in terms of proposed nanoparticles mechanisms. The first is that nanoparticles can prevent droplet coalescence as shown in the oil drop behavior experiment, section 4.4. The purported mechanism is that a portion of the hydrophilic silica

nanoparticles gather at the interface between oil and water and act as a shield preventing the water phase from getting in contact with the oil phase (Dickson, 2004). This matches the results seen here.

The second concerns the wettability changes caused by some, but not all, of the nanoparticles tested. The wettability change caused by the nanoparticle solutions could be attributed to various factors. The injection of the hydrophilic nanofluids to the system has been noticed to change the contact angle towards the water and intermediate wetness range, cause the oil drop to completely snap off the surface, and to wedge off a big portion of the drop and change the contact angle of the remaining portion.

The wedging and cutting of the oil drops by nanofluids, which is the second mechanism, shown in the experiments of this study represent some compliance with the wetting and spreading phenomena of colloidal fluids containing nanometer-sized particles that was discussed by Wasan et al. (2011). The ordering of the nanofluids inside a confined geometry of the wedge film formed between an oil drop and a solid surface increases the entropy of the nanoparticles as greater freedom is permitted. As a result, an excess pressure which is referred to as the disjoining pressure would be exerted which will separate the oil drop and help spread the nanoparticles layer on the surface towards the wedge vertex. Figure 4-57 illustrates the hypothesized wedge film and structural disjoining pressure caused by nanoparticles.

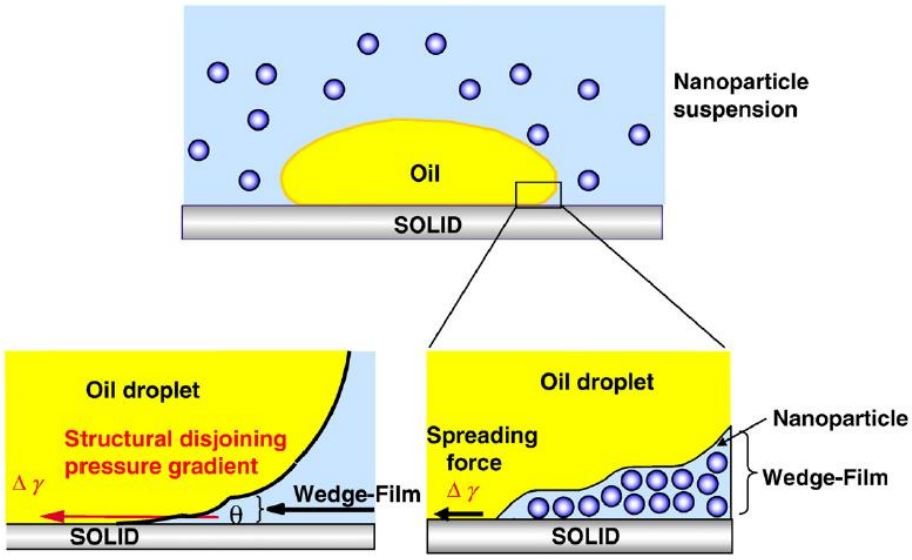

Figure 4-57: Wedge film that causes the structural disjoining pressure (Wasan, 2011)

On the other hand, grafting or coating nanoparticles with certain chemicals polyethylene glycol along with suspending them in solutions that may contain some surfactant would definitely have an effect on the wettability and IFT. All of the nanofluids used in this study's experiments contain silica nanoparticles, yet the wedging and wettability alteration behaviors have not been the same. The nanoparticles coating in these samples and the chemical mixtures in the carrying solution are different, which justifies the controversy in the results and emphasizes the importance of these chemical components in altering the surface wettability and IFT. Moreover, the secrecy measures taken by the nanofluids manufacturers about the exact chemical content hindered the study from further understanding nanofluids effects on wettability.

Nissan nanoparticles showed no IFT change, but changed the contact angle. This would make sense for a wedging hypothesis as they are forcing themselves to the water/oil interface which will exert the necessary pressure to change the contact angle and/or snap off the oil droplet at certain conditions as shown above. On the other hand, Company X

nanoparticles showed both IFT changes and contact angle changes. This would suggest that the particles may be wedging, but the reduction of oil/water IFT will also change contact angle as illustrated in Figure 4-58 where interfacial forces and the contact angle are noted. Based on this analysis, the change in wettability is a factor of both the nanoparticles wedging and the reduction in IFT which is caused by the chemicals grafted on the particles surface and mixed in the carrying solution.

By balancing the interfacial forces indicated on Figure 4-58, we obtain the following equation to relate contact angle through the water phase and the remaining three interfacial tensions between water, oil and the solid plate (γ_{wo}, γ_{so}, and γ_{sw}):

$$cos\theta_w = \frac{\gamma_{so} - \gamma_{sw}}{\gamma_{wo}}$$

Initially, the contact angle is higher than 90° before adding nanoparticles which represent an oil-wet state. After adding nanoparticles, certain samples such the samples from Company X, reduced the water/oil IFT and reduced the contact angle where it became less than 90° which represent a water-wet state. If we assume that the added nanoparticles have only reduced the water/oil IFT while keeping the other two IFTs constant (γ_{so} and γ_{sw}), the oil contact angle should increase as per the force balance equation above which means that the rock surface should become more oil-wet; however, this is not observed in the experiments where the contact angle became less than 90° which represents a water-wet state.

This leaves us with two hypotheses into how is the wettability affected with nanoparticles. The first is the abovementioned wedging by nanoparticles. The second is adsorption of the particles or the chemicals around the particles on the mineral surface which can alter the other interfacial forces and the contact angle drastically. The second

hypothesis is assumed after ruling out the water/oil IFT reduction factor in altering wettability and using surfactants adsorption and wettability alteration capability as an analogy which is explained by Somasundaran and Zhang (2006). Moreover, the nanoparticles adsorption experiments mentioned by Zhang (2015) supports our second wettability alteration hypothesis of particles adsorption.

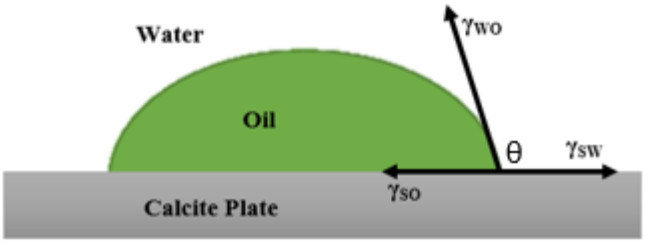

Figure 4-58: Interfacial tensions between three phases and the contact angle

Chapter 5: Conclusions and Future Work

Changing the rock surface wettability from oil-wet to water-wet proved oil recovery enhancement in previous studies. Moreover, most of the carbonate reservoirs around the world are oil-wet, which motivates the research toward finding means to alter carbonates wettability into water wetness. In addition, reducing interfacial tension between oil and water has beneficial effects to mobilize residual or trapped oil, which will increase the overall cumulative production. Also, silica nanoparticle solutions have shown some promising signs regarding oil recovery enhancement and CO_2 sequestration projects, which triggered the research interest to study the effects of various nanoparticle solutions on carbonates wettability and oil/water interfacial tension.

5.1 Conclusions

Changing carbonates surface wettability toward a water-wet range is possible. However, the existence of the suspended silica nanoparticles is not the main factor in altering wettability as noticed in the previous experiments. The chemicals grafted on the nanoparticles surface or mixed in the carrying solution are supporting the wettability alteration process. Moreover, the known chemical components used in the nanoparticle samples are ethylene glycol, polyethylene glycol and GLYMO. The exact chemical content is only known for the nanoparticle solutions synthesized in-house.

Nissan nanoparticle solutions did not affect the wettability at the early experiments which is attributed to particles stability issues even though most of their samples did not show any significant aggregation signs as only slight cloudiness appeared at the lower side of the cuvette. Moreover, resolving the stability issues of the Nissan nanoparticles by reducing the solution's pH resulted in changing the wettability toward an intermediate range (80° - 100°) at 1% nanoparticles concentration. IFT has minimally changed using

Nissan nanoparticles. On the other hand, Company X nanoparticles altered both wettability and IFT significantly where contact angles changed toward the water-wet range (<100°) and IFT values reduced to 6 dynes/cm (initially 28 dynes/cm).

Some of the used nanoparticle samples did not have any significant effect on contact angles or IFT such as the case with the NYACOL sample. The in-house synthesized nanoparticles with polyethylene glycol changed the contact angle toward an intermediate wettability range (98°) and the IFT reduced by 43%. In contrast, the synthesized nanoparticle solution with GLYMO showed no signs of wettability alteration, but reduced brine/oil IFT by 24%. Overall, samples that affected wettability and IFT showed greater effects at higher concentrations; however, using nanoparticles at high concentrations might not be economically viable.

Introducing certain nanoparticle solutions at 1% concentration to the system caused oil drops to snap off the surface completely or partially along with a change in contact angles of the remaining oil portions. Snapping off and contact angle alteration are possibly occurring due to the nanoparticles order around the oil/water interface which is explained by the wedging hypothesis in the previous chapter, or the chemicals on the nanoparticles surface and in the carrying solution that can adsorb on the mineral surface.

5.2 Recommendations and Future Work

To get a better understanding of the physics and main factors behind wettability and IFT alterations using hydrophilic silica nanoparticles, a full knowledge of the chemical content and surface coating is necessary (to be obtained from commercial producers). Moreover, the in-house synthesized nanoparticle solutions would be the best to experiment on due to the full control over the added chemical components. Also, the wettability and IFT experiments can be done at higher temperatures using electrical heating pads below

the cuvette to simulate change under reservoir temperatures. In addition, core wettability can be evaluated by generating drainage and imbibition curves under similar conditions to ensure applicability and efficiency in carbonate reservoir floods. Finally, adsorption experiments in carbonate cores will also help a better understanding of nanoparticles mechanisms in altering wettability.

References

Abdallah et al. 2007. Fundamentals of Wettability. *Schlumberger Oilfield Review*. Schlumberger Wettability Workshop-Bahrain. May. 44-61.

Anderson, W. G. 1986. Wettability Literature Survey-Part 1: Rock/Oil/Brine Interactions and the Effects of Core Handling on Wettability. *Journal of Petroleum Technology*. 38. 1125-1144. SPE 13932.

Anderson, W. G. 1986. Wettability Literature Survey-Part 2: Wettability Measurement. *Journal of Petroleum Technology*. 38. 1246–1262. SPE 13933.

Anderson, W. G. 1986. Wettability Literature Survey-Part 3: The Effects of Wettability on the Electrical Properties of Porous Media. *Journal of Petroleum Technology*. 38. 1371-1378. SPE 13934.

Anderson, W. G. 1987. Wettability Literature Survey Part 4: Effects of Wettability on Capillary Pressure. *Journal of Petroleum Technology*. 39. 1283–1300. SPE 15271.

Anderson, W. G. 1987. Wettability Literature Survey Part 5: The Effects of Wettability on Relative Permeability. *Journal of Petroleum Technology*. 39. 1453–1468. SPE 16323.

Anderson, W. G. 1987. Wettability Literature Survey Part 6: The Effects of Wettability on Waterflooding. *Journal of Petroleum Technology*. 39. 1605–1622. SPE 16471.

Aroonsri, A., Worthen, A., Hariz, T., Johnston, K., Huh, C. and Bryant, S. 2013. Conditions for Generating Nanoparticle-Stabilized CO2 Foams in Fracture and Matrix Flow. *SPE Annual Technical Conference and Exhibition – New Orleans, Louisiana, USA*. SPE 166319

Austad, T., Strand, S., Madland, M. V., Puntervold, T., and Korsnes, R. I. 2008. Seawater in Chalk: An EOR and Compaction Fluid. *SPE Reservoir Evaluation and Engineering*. 11(04). 648–654. SPE 118431.

Chatzis, I., and Morrow, N. R. 1984. Correlation of Capillary Number Relationships for Sandstone. *Society of Petroleum Engineers Journal*. 24(05). 555-562. SPE 10114.

Dickson, J. L., Binks, B. P., and Johnston, K. P. 2004. Stabilization of Carbon Dioxide-in-Water Emulsions with Silica Nanoparticles. *American Chemical Society-Langmuir*. 20. 7976-7983.

Firoozabadi, A., and Ramey, H. J. 1988. Surface Tension of Water-Hydrocarbon Systems at Reservoir Conditions. *Journal of Canadian Petroleum Technology*. 27(03). 41-48.

Horikoshi, S., and Serpone, N. 2013. Introduction to Nanoparticles. Microwaves in Nanoparticle Synthesis. Weinheim, Germany: Wiley-VCH.

Ju, B., and Fan, T. 2009. Experimental Study and Mathematical Model of Nanoparticle Transport in Porous Media. *Powder Technology*. 192. 195-202.

Ju, B., Fan, T., and Ma, M. O. 2006. Enhanced Oil Recovery by Flooding with Hydrophilic Nanoparticles. *China Particuology*. 4(01). 41-46.

KRUSS. 2016. Pendant Drop. Retrieved on 28 May, 2016 from: http://www.kruss.de/services/education-theory/glossary/pendant-drop/

Kumar, K., Dao, E. K., and Mohanty, K. K. 2008. Atomic Force Microscopy Study of Wettability Alteration by Surfactants. *Society of Petroleum Engineers Journal*. 13(02). 137-145. SPE 93009.

Ogolo, N. A., Olafuyi, O. A., and Onyekonwu, M. O. 2012. Enhanced Oil Recovery Using Nanoparticles. *SPE Saudi Arabia Section Technical Symposium and Exhibition – Al-Khobar, Saudi Arabia*. SPE 160847.

Onyekonwu, M. O., and Ogolo, N. A. 2010. Investigating the Use of Nanoparticles in Enhancing Oil Recovery. *Annual SPE International Conference and Exhibition – Tinapa, Calabar, Nigeria*. SPE 140744.

Owens, W. W., and Archer, D. L. 1971. The Effect of Rock Wettability on Oil-Water Relative Permeability Relationships. *Journal of Petroleum Technology*. 23(07). 873–878. SPE 3034.

Peters, E. J. 2012. Interfacial Phenomena and Wettability. Advanced Petrophysics (Vol. 2). Austin, Texas, USA: Live Oak Book Company.

Pope, G. A., Wu, W., Narayanaswamy, G., Delshad, M., Sharma, M. M., and Wang, P. 2000. Modeling Relative Permeability Effects in Gas-Condensate Reservoirs with a New Trapping Model. *SPE Reservoir Evaluation & Engineering*. 3(02). 171–178. SPE 62497.

Raza, S. H., Treiber, L. E., and Archer, D. L. 1968. Wettability of Reservoir Rocks and Its Evaluation. *Producers Monthly*. 32(04). 2-7.

Research Gate. 2007. The Actual and the Apparent Contact Angle on a Rough Surface. Retrieved on 28 May, 2016 from: https://www.researchgate.net/278663692_fig27_Figure-31-24-The-actual-and-the-apparent-contact-angle-on-a-rough-surface

Rosen, M. J., Wang, H., Shen, P., and Zhu, Y. 2005. Ultralow Interfacial Tension for Enhanced Oil Recovery at Very Low Surfactant Concentrations. *American Chemical Society - Langmuir*. 21. 3749-3756.

Roustaei, A., and Bagherzadeh, H. 2013. Experimental Investigation of SiO_2 Nanoparticles on Enhanced Oil Recovery of Carbonate Reservoirs. *Journal of Petroleum Exploration and Production Technology*. 5. 27-33.

Roustaei, A., Moghadasi, J., Bagherzadeh, H., and Shahrabadi, A. 2012. An Experimental Investigation of Polysilicon Nanoparticles' Recovery Efficiencies through Changes in Interfacial Tension and Wettability Alteration. *SPE International Oilfield Nanotechnology Conference and Exhibition - Noordwijk, The Netherlands*. SPE 156976.

Sheng, J. 2010. Modern Chemical Enhanced Oil Recovery: Theory and Practice. Amsterdam, Netherlands: Elsevier Science Company.

Skauge, T., Hetland, S., Spildo, K., and Skauge, A. 2010. Nano-sized Particles for EOR. *SPE Improved Oil Recovery – Tulsa, Oklahoma, USA*. SPE 129933.

Somasundaran, P., and Zhang, L. 2006. Adsorption of surfactants on minerals for wettability control in improved oil recovery processes. *Journal of Petroleum Science and Engineering*. 52. 198–212.

Standnes, D. C., and Austad, T. 2000. Wettability Alteration in Chalk: Mechanism for Wettability Alteration from Oil-wet to Water-wet Using Surfactants. *Journal of Petroleum Science and Engineering*. 28. 123-143.

Taber, J. J. 1969. Dynamic and Static Forces Required to Remove a Discontinuous Oil Phase from Porous Media Containing Both Oil and Water. *SPE European Regional Meeting – Milano, Italy*. SPE 2098.

Treiber, L. E., Archer, D. L., and Owens, W. W. 1972. A Laboratory Evaluation of the Wettability of Fifty Oil-Producing Reservoirs. *Society of Petroleum Engineers Journal*. 12. 531-540. SPE 3526.

Tweheyo, M. T., Zhang, P., and Austad, T. 2006. The Effects of Temperature and Potential Determining Ions Present in Seawater on Oil Recovery from Fractured Carbonates. *SPE Improved Oil Recovery – Tulsa, Oklahoma, USA*. SPE 99438.

Ward's Science. 2016. Calcite (Iceland Spar). Retrieved on 28 May, 2016 from: https://www.wardsci.com/store/product/8868921/calcite-iceland-spar

Wasan, D., Nikolov, A., and Kondiparty, K. 2011. The Wetting and Spreading of Nanofluids on Solids: Role of the Structural Disjoining Pressure. *Current Opinion in Colloid & Interface Science*. 16. 344-349.

Xu, K., Zhu, P., Huh, C., and Balhoff, M. T. 2015. Microfluidic Investigation of Nanoparticles' Role in Mobilizing Trapped Oil Droplets in Porous Media. *American Chemical Society - Langmuir*. 31. 13673-13679.

Xu, K., Zhu, P., Huh, C., and Balhoff, M. T. 2015. Microfluidic Investigation of Nanoparticles' Role in Mobilizing Trapped Oil Droplets in Porous Media. *American Chemical Society - Langmuir*. 31. 13673-13679.

Yousef, A. A., Al-Saleh, S., Al-Kaabi, A., and Al-Jawfi, M. 2010. Laboratory Investigation of Novel Oil Recovery Method for Carbonate Reservoirs. *SPE Canadian Unconventional Resources & International Petroleum Conference – Calgary, Alberta, Canada*. SPE 137634.

Zhang et al. 2015. Investigation of Nanoparticles Adsorption during Transport in Porous Media. *Society of Petroleum Engineers Journal*. 20(04). 667-677.

Zhang, D. L., Liu, S., Puerto, M., Miller, C. A., and Hirasaki, G. J. 2006. Wettability Alteration and Spontaneous Imbibition in Oil-wet Carbonate Formations. *Journal of Petroleum Science and Engineering*. 52. 213–226.

Vita

Hamdi Alramadan was born in Dhahran, Saudi Arabia. After graduating from high school, he entered the college preparatory program of the national oil company, Saudi Aramco, in 2006. He entered Colorado School of Mines in 2007 and received the degree of Bachelor of Science in petroleum engineering with honors in May 2011. He interned for Schlumberger Data and Consulting Services in Denver, Colorado during the summer of 2010. During the following years, he was employed as a reservoir engineer at Saudi Aramco's reservoir management sector. He was also assigned as a production engineer for a full year in 2013. In August, 2014, he entered the Graduate School at the University of Texas at Austin.

Permanent email address: myhamdi2007@gmail.com

This thesis was typed by the author.